molecules

MDPI

Review

Recent Advances in the Synthesis of Inorganic Materials Using Environmentally Friendly Media

Lorenzo Gontrani [1,2,*], Pietro Tagliatesta [1], Domenica Tommasa Donia [3], Elvira Maria Bauer [4], Matteo Bonomo [2,5] and Marilena Carbone [1,*]

1 Department of Chemical Science and Technologies, University of Rome Tor Vergata, Via della Ricerca Scientifica 1, 00133 Rome, Italy; pietro.tagliatesta@uniroma2.it
2 Department of Chemistry, University of Rome "La Sapienza", P.le A. Moro 5, 00185 Roma, Italy
3 Department of Surgical Science, University of Rome Tor Vergata, Via Montpellier 1, 00133 Rome, Italy; donia@med.uniroma2.it
4 Italian National Research Council-Institute of Structure of Matter (CNR-ISM), Via Salaria km 29.3, 00015 Monterotondo, Italy; elvira.bauer@mlib.ism.cnr.it
5 Department of Chemistry, NIS Interdepartmental Centre and INSTM Reference Centre, University of Turin, Via Pietro Giuria 7, 10125 Turin, Italy; matteo.bonomo@unito.it
* Correspondence: lorenzo.gontrani@uniroma2.it (L.G.); carbone@uniroma2.it (M.C.)

Abstract: Deep Eutectic Solvents have gained a lot of attention in the last few years because of their vast applicability in a large number of technological processes, the simplicity of their preparation and their high biocompatibility and harmlessness. One of the fields where DES prove to be particularly valuable is the synthesis and modification of inorganic materials—in particular, nanoparticles. In this field, the inherent structural inhomogeneity of DES results in a marked templating effect, which has led to an increasing number of studies focusing on exploiting these new reaction media to prepare nanomaterials. This review aims to provide a summary of the numerous and most recent achievements made in this area, reporting several examples of the newest mixtures obtained by mixing molecules originating from natural feedstocks, as well as linking them to the more consolidated methods that use "classical" DES, such as reline.

Keywords: Deep Eutectic Solvents; nanoparticles; inorganic synthesis; environmentally friendly media; biocompatibility; renewable feedstocks

Citation: Gontrani, L.; Tagliatesta, P.; Donia, D.T.; Bauer, E.M.; Bonomo, M.; Carbone, M. Recent Advances in the Synthesis of Inorganic Materials Using Environmentally Friendly Media. *Molecules* **2022**, *27*, 2045. https://doi.org/10.3390/molecules27072045

Academic Editors: Mara G. Freire and Santiago Aparicio

Received: 25 February 2022
Accepted: 18 March 2022
Published: 22 March 2022

1. Introduction

According to the general definition currently used (EU 2011), a "nanoparticle" (NP) is a discrete (nano-)object where at least one of its characteristic dimensions falls in the range 1–100 nm. This category thus includes objects with a fixed number of such dimensions, such as nanowires/nanotubes (mono-dimensional, 1D) and nanodiscs/nanoplates (2D), as well as nanometric spherical/globular three-dimensional aggregates. Nanoparticles can be further classified according to their organic/inorganic nature. Dendrimers, lyposomes, and polymeric NPs belong to the former group, whereas fullerenes, quantum dots, and metal/metal oxide NPs to the latter [1,2]. Most importantly, nanomaterials are classified according to their size, shape, and properties, and it is this last feature that has led to the blossoming of nanomaterial research in the last few years. The remarkable properties nanoparticles possess (e.g., optical, magnetic, and electrical) can be exploited in a large number of technology-related fields, ranging from electronics [3,4] to biology and medicine [5,6]. The correlation between size/shape and properties in nanomaterials was thoroughly assessed in several investigations, and it was shown that their properties were dramatically dependent on the shapes, dimensions, and porosities of the synthesized nanoobjects; thus, a detailed control of the synthetic route is needed. The structural differences observed ultimately result in remarkably different performances in real-world

applications. Among the factors that can be controlled, the most easily tunable is probably temperature. For instance, in the synthesis of metal oxides by the co-precipitation pathway, the temperature at which the drying/calcination of the hydroxide is carried out can vary widely. Despite its apparent "simplicity", the effect of this variation can be quite relevant, as was found, for instance, in the synthesis of nickel (II) oxide NiO, a prototypical p-type, wide-band-gap semiconductor. NiO nanoparticles prepared at 400 °C are smaller and more porous, while larger structures are obtained at 600 °C; the band gaps associated with the latter are larger and the electrochemical performances worse, especially when these nanoparticles are introduced into screen-printed electrodes (SPEs) and employed as electrochemical sensors for selective assays or in Faradic pseudo-capacitors. Other factors that have been found to influence the intercalation of precursors and the sintering of particles, the latter leading to particles of larger sizes, are the reagents used to prepare the precursor hydroxide $Ni(OH)_2$: the use of various combinations of nickel salts and inorganic/organic bases as precipitating agents, and the adoption of surfactant-free hydrothermal synthesis or microwave irradiation (which can lead to different results) [7–12].

In a large number of studies aiming to control the shape and dimensions of particles, the use of templating agents has been investigated in more detail. Various types of systems have been employed for this purpose, such as, for instance, boric, citric, and ascorbic acids [13]; cholesteric liquid crystals [14]; and different types of surfactants [15]. Here, the use of dendrimers such as poly(amidoamine) (PAMAM) is noteworthy, as it allowed the production of very small NPs with dimensions as low as 1.4 nm [16]. In this contribution, we focus our attention on a new class of environmentally friendly, inherently inhomogeneous, and highly structured family of liquids, Deep Eutectic Solvents, which can naturally exert a templating effect. The most recent developments in the field will be reviewed and additional references will be provided, thus enlarging the literature coverage of the reviews already published on this subject [17–20].

2. Brief Description of Deep Eutectic Solvents

Since the "official" birthday of this family of liquids, which can be traced back to the pivotal paper by Abbott in 2003 [21], a fairly large amount of research has been dedicated to them, especially in the last decade. The key feature of these solvents is their very easy and economic preparation, which involves the simple mixing of at least one hydrogen bond donor (HBD) with at least one hydrogen bond acceptor (HBA). In most cases, this takes place in solid phase and in definite ratios, providing mixtures with remarkably lower melting points than those of their individual components. The sometimes very large decrease seen in the melting temperature, which in the prototypical choline chloride:urea 1:2 system ("Reline") [22] can be more than 100 °C with respect to the ideal value obtainable from thermodynamics arguments [23,24], has led to the term "deep" being used to distinguish DESs from other non-ideal physical systems where similar phenomena are observed—e.g., water–DMSO mixtures. Deep Eutectic Solvents were divided into four main classes in the original classification by Abbott, three of which contain a halide anion and a quaternary ammonium cation as HBA (in most cases, choline chloride), and differ in their type of HBD: metal chloride in class I, hydrated metal chloride in class II, organic molecules (such as urea, glycerol, and carboxylic acids) in class III (which is the most populated), and metal halides and urea (or acetamide/ethylene glycol) in class IV. Recently, a new class was introduced ("type V" [25]), containing only hydrogen-bond donors and acceptors and no ions. Other non-negligible valuable traits of Deep Eutectic Solvents are their high sustainability, especially in the subfamily NaDES (Natural DES), where the precursors are benign compounds generally obtained from natural feedstocks, such as choline chloride and carboxylic acids; these therefore have a low toxicity and high biocompatibility and biodegradability [26–28]. Additionally, DESs are characterized by their high conductivities, viscosities, and surface tensions; have a low volatility and flammability; and have highly tunable physiochemical properties, considering the large number of possible combinations of precursor salts [29]. These last features are shared with ionic liquids (ILs), which can

be considered as the forefathers of DESs. However, ILs are composed (almost entirely) of ions [30,31], whereas DESs, apart from the type V ones, are mixtures that contain polar molecules and ions. A sketch of the desirable technological properties of DESs is provided in Figure 1.

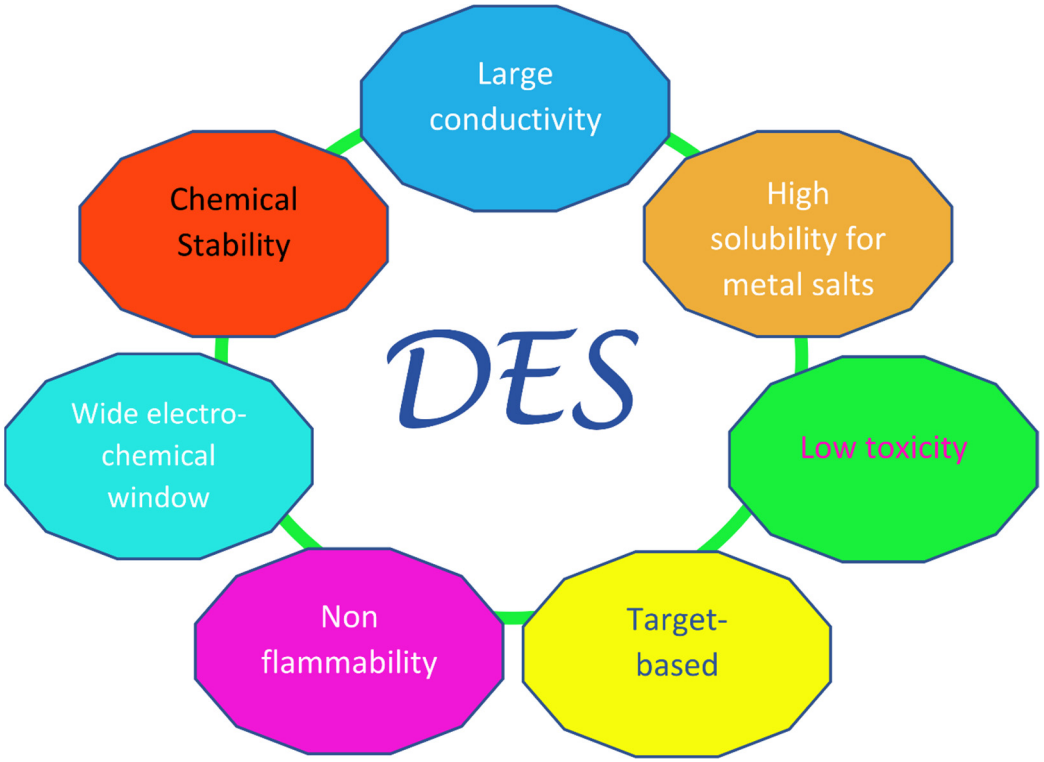

Figure 1. Pictorial diagram of the innovative properties of Deep Eutectic Solvents, inspired by Ref. [29].

3. DES in Nanoparticle Synthesis from Their Birth to 2020

The investigation of the applicability of ILs and DESs in the field of nanoparticle synthesis started with a focus on the former family, but the amount of research on DES has been growing lately. In addition, some of the features characteristic of ILs can be extended seamlessly to DESs. The most striking property of DESs in the field of nanoparticle synthesis is the high solubility of metal ion salts and complexes in several cases. As already shown by Abbott et al. [32], the solubility of some bulk metal oxides, which are almost insoluble in pure water, is greatly increased in some DESs, reaching values of up to more than 10,000 parts per million in ChCl:malonic acid 1:1 at 50 °C for Cu_2O, CuO, and ZnO, and up to 90,000 ppm for ZnO in ChCl:urea 1:2 at 70 °C. In contrast, other oxides, such as iron oxides, are barely soluble in ChCl:urea 1:2. This feature can be used, for instance, to design suitable synthesis protocols based on fractional precipitation. Another key factor is the possibility of these substances acting in a dual capacity as both solvents and templates for nanostructure formation ("target solvent") [33–37], owing to their structural heterogeneity [38–41]. In several cases, DESs can behave as reactants as well [42–44].

The heterogeneity and microstructure of DESs have attracted great interest. The study by Chen et al. [45] pointed out that in "reline" (ChCl:urea 1:2), "ethaline" (ChCl:ethylene glycol 1:2), and "glyceline" (ChCl:glycerol 1:2 (the classification of this mixture as a DES or as a salt-in-solvent system has recently been debated, and the data are in favor of a 1:3 composition defining a proper DES [46])), the charged and neutral portions of the mixtures tend to separate when the liquid comes into contact with graphite electrodes, with choline and chloride ions being attracted into the Stern layer, while the molecular components are excluded at all the potentials scanned. Similar experiments carried out using Pt(111) electrodes and the same three DESs were conducted at various potentials and at increasing

water contents [47]. This study showed that the addition of water in amounts up to ≈40 wt% did not lead to the decomposition of the interfacial nanostructure, as observed in ILs even at very small water contents. Yet, the cyclic voltammetry analysis reported in the same study indicates that, at such high water concentrations, the nanostructure appears comparable to that of salt solutions. The preservation of the microscopical structure upon hydration was also demonstrated in a neutron diffraction study conducted by Hammond et al. [48], who pointed out that the microscopic features of pure reline were maintained in a water to DES molar ratio of up to 10:1 (around 42 wt% H_2O); beyond that limit, the system can be better described as a three-component HBA:HBD:water mixture. Marked heterogeneity was evidenced as well in a molecular dynamics study conducted by Alizadeh et al. [34], who reported the fate of ethaline's polar and nonpolar molecular groups under electrostatic potential. The calculations suggest that the DES reorganizes in order to maximize the interactions between domains of the same polarity, thus inducing strong heterogeneity in the system.

The oldest syntheses reported mainly concerned the preparation of noble metal nanoparticles with a controlled shape; in most cases, these syntheses employed Abbot's DES reline [21]: catalysts containing star-like gold NPs were synthesized through the reduction of $HAuCl_4$ by L-ascorbic acid in DES without surfactants or seeds at room temperature ([49], see Figure 2). The shape could be further changed (e.g., to a snowflake or nanothorn) by adjusting the water content. Other noble metal NPS were prepared by electrosynthesis methods: in this regard, DESs can be very valuable, since they possess very wide electrochemical windows just slightly bit smaller than ILs which can be effectively coupled to the large solubility of metal oxides to set up electrochemical cells for the deposition of metal nanoparticles, achieving very efficient control over the nucleation, deposition rate, and size of the crystals obtained [50]. A further very important aspect of noble metal deposition is that DES and ILs can substitute highly toxic cyanide-based electrolytes [51]. Among these examples, the preparation of concave tetrahexahedral Pt nanocrystals by electrodeposition using reline without employing surfactants, seeds, or other chemicals but with a high control of the shape and a high surface energy was reported [52]. Two-dimensional superstructures of aggregated Pd nanoparticles were electrodeposited from choline chloride:urea 1:2 onto glassy carbon foil, with the absorbed species forming an anionic layer that was observed with Ultra Small X-Ray Scattering (USAXS) [53]. Platinum icosahedral nanocrystals with high-index facets and a higher electrocatalytic activity and stability were electro-synthesized in reline [54]. Further details on the role of Deep Eutectic Solvents in the synthesis of plasmonic (Au, Ag, Pt) nanoparticles can be found in the recent review of Des et al. [55], who also describe biocompatible capping strategies that make use of polysaccharides (carrageenan), resulting in highly monodisperse nanoparticles. Other non-electrochemical redox reactions were carried out using environmentally friendly routes based on reline as a solvent: CuCl nanocrystal powder, which is a very useful catalyst for organic synthesis, was obtained either through the synproportion of $CuCl_2$ and Cu [56] or by the reduction of $CuCl_2$ by ascorbic acid [57]. Additionally, spherical, magnetic nanoparticles of ferrous ferrite (Fe_3O_4) were prepared at 80 °C and successfully tested for the absorption of Cu^{2+} ions, proving to be superior to NPs prepared in pure water [58]. Further examples of systems prepared in reline with co-precipitation are PbS nano/micro superstructures made from lead (IV) and thioacetamide [59], mesoporous NiO [60], and some examples of iono-thermal reactions at high temperatures/pressures (nanoflower-like α-$Ni(OH)_2$ and NiO [61], Ni_2P supported on amorphous/mesoporous $Ni_3(PO_4)_2$-$Ni_2P_2O_7$ [62], nanosized SnO crystals [63], Fe_2O_3 nanospindles as high-capacity anode materials [64], mesoporous Co_3O_4 sheets or nanoparticles [65], and $MnCO_3$/MnOx mesocrystals [66]). An interesting example of an "antisolvent approach" is the synthesis of ZnO nanocrystals doped with Cu(II) ions, which involves adding a controlled amount of water to solutions of bulk ZnO in DES [67]. Few studies have employed DESs other than reline; some noteworthy examples utilize ethylene glycol as the HBD partner of ChCl, the latter being used to obtain nanocrystalline SnO_2 or SnO_2/graphene nanocomposites [68],

nanoporous Ag films [69], and Ni-P alloy nanoparticles [70] to deposit Ni deposits [71], Ni-Ti nanocomposite coatings [72], or Ag films [73]. In an interesting study by Mota-Morales [74], the dispersant properties of DESs during the formation of nanoparticles and other nanocomposites were exploited for the preparation of a microporous carbon nanotube-polyacrylic acid composite using a ChCl:acrylic acid mixture. The latter DES was also successfully employed as a functional monomer to create DES-levofloxacin-imprinted Pd nanoparticles for the selective removal of pollutants from wastewater [75].

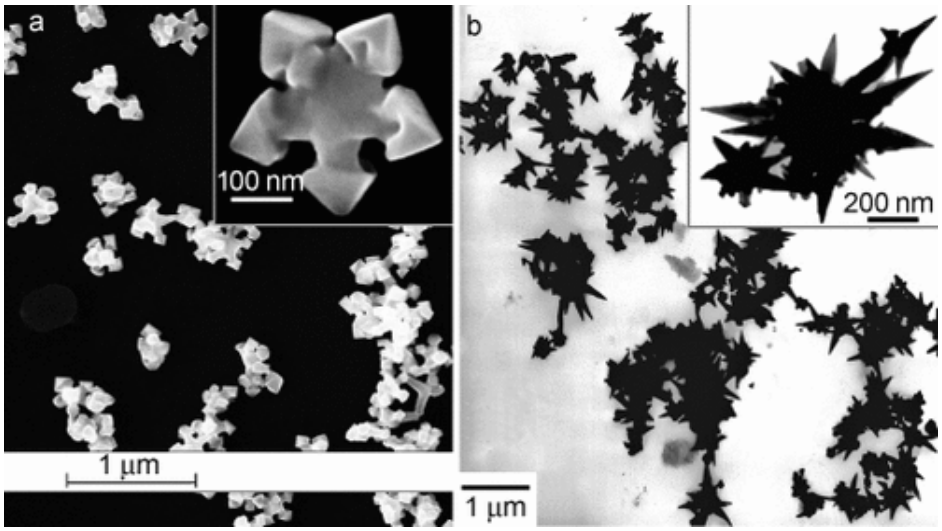

Figure 2. Deep Eutectic Solvents as green media in the synthesis of anisotropic Au nanoparticles (panel (**a**): flower shape; panel (**b**): nanothorn). Reproduced with permission from ref. [49]. Copyright 2008 John Wiley and Sons.

More recently, the increasing need for even greener and more biocompatible alternatives has fostered the usage of new types of environmentally benign and low-cost mixtures, mostly belonging to the NADES family (DESs of natural origin), where the precursors are obtained from renewable feedstocks. For instance, Zainal-Abidin et al. recently reported that graphene is significantly less cytotoxic when it is functionalized with ChCl:glucose/fructose/sucrose) 2:1 or, better yet, ChCl:malonic acid 1:1, with respect to pristine or oxidized graphene owing to surface modifications [76]. NADES mixtures containing glucose, fructose, and sucrose as HBD, choline chloride, and water at different molar ratios, were employed in the synthesis of MoS_2 nanosheets by Mohammadpour et al. [77]. The material prepared was stable in aqueous environments, could perform as a catalyst in hydrogen evolution reactions (HERs), and could be obtained in a higher yield compared to other exfoliating agents (average of 44% vs. 20%). New mixtures created by changing the HBA or HBD started to be explored in the last part of the 2010s: an interesting example of those belonging to the second group is the synthesis of calcite nanoparticles by the reaction of CO_2 with "calcoline", a DES composed of choline chloride and calcium chloride [78]. This study demonstrates that DESs can be successfully exploited in "carbon-reduction" protocols, leading to value-added products. A modification of the acceptor moiety (HBA) was used by Adhikari et al., who reported the use of halide-free DES, where the Cl-anion of reline is replaced by nitrate, for the microwave-assisted reduction of silver salts to organic-soluble oleylamine-capped Ag nanoparticles [79]. Following on from this study, Adhikari et al. later fine-tuned a silver-based DES (1:4 silver triflate:acetamide, "argentous DES") that allowed them to obtain large amounts of monodispersed colloidal silver nanocrystals of high quality despite the high metal concentration, owing to the "size focusing" effect of the DES that suppressed uncontrolled nanocrystal growth [80]. More recently, these researchers exported their methodology to flow-reactor synthesis employing dimethylammonium nitrate-polyol DES media; they were able to obtain a 1000- to 4000-fold increase in throughput compared to conventional synthesis [81]. Other noteworthy examples of HBA

modifications include mixtures of non-quaternary cations, such as dimethylamine, ethylamine, and trimethylamine hydrochlorides with urea, which have been successfully used to synthesize a series of silver and selenido-stannate ($[NH_2(CH_3)_2]_2Sn_3Se_7 \cdot 0.5NH(CH_3)_2$, $[NH_4]_2Sn_4Se_9$, $[NH_3C_2H_5]_2Sn_3Se_7$, and $[NH_4]_3AgSn_3Se_8$) crystals through the solvothermal pathway. The ammonium cations originating from the original HBA as well as those resulting from the decomposition of urea have been proven to be able to act as templating agents, leading to the establishment of three-dimensional supermolecular inorganic frameworks that show the peculiar feature of thermochromism in some cases [82]. The use of ammonium cations as hydrogen bonds, though very common and convenient, is not the only option. In fact, other inorganic salts have recently been used. For example, ionic compounds belonging to the alkali halide family have been proven to form polyol-based DES mixtures (such as CsF/KF:glycerol) that have shown very high selectivities when used as reaction media for copper-catalyzed homocoupling organic reactions [83].

Returning to DESs containing molecules of natural origin, a mixture of caffeic acid with ChCl and ethyleneglycol was used to prepare moleculary imprinted hexagonal boron nitride NPs, which were successfully employed in the solid-phase extraction of flavonoids [84], while tartaric acid was used as a DES component in a recent electrodeposition preparation of a Ti/SnO_2–Sb electrode with a high electrochemical activity [85].

In summary, the main advantages of DES that were readily highlighted shortly after their introduction as synthesis media and that were largely demonstrated during this initial time period lie in their friendliness towards ecosystems, their highly tunable physiochemical properties, and their cheap means of preparation and handling. An additional very important and profitable feature is their intrinsic microheterogeneity, with it being possible to confer specific morphologies to the obtained nanoparticles. A possible drawback of the use of DESs is their moderate viscosity, which depends on the nature of their components, with the viscosity being lower for hydrophobic DESs and larger for sugar-based NADESs. Indeed, it has been shown that the decrease in mass diffusivity caused by viscosity affects nanoparticle growth and generally leads to NPs of a larger size [86].

4. Research on DES Blooms: From 2020 up to Now

The number of investigations on a multifaceted topic such as DES have increased markedly in the last few years. The simple query "Deep Eutectic Solvents" in the title, abstract, and keywords on Scopus database yielded 6474 results on 17 February 2022; a more refined inquiry ("deep eutectic solvents" AND "nanoparticles") on the same day led to 343 results, 22 of which were published in the first fifty days of 2022. The full set of trends discovered is shown below (Figure 3). During the last two years, research in this field has continued in the direction of considering new eutectic mixtures that are often cheap and biocompatible. The published studies include "wet chemistry" synthesis protocols (i.e., synthetic routes not assisted by electrochemical methods or other instrumentations, such as CVD; see Table 1 for a schematic report) as well as electrochemical deposition methods, which have already been proven to be very efficient in producing several types of nanoparticles. Among all the literature, although reline still plays an important role (since it features in approximately one out of four studies (80/343) on both traditional liquid-phase syntheses and electrodeposition), the interest in new methods has grown significantly and NADESs are becoming more and more important every day. Among the newest and most interesting investigations using "traditional" ChCl:urea, the latter DES was used: in the field of metal oxides synthesis, to prepare nontoxic photoluminescent SnO nanoparticles for cell imaging [87], in the solvothermal synthesis of iron oxide from iron monitored in operando by SANS and EXAFS [88], in the synthesis of ceria nanoparticles in a continuous microreactor [89], to conjugate Fe_3O_4 nanoparticles on graphene oxide [90], to obtain $NixCo_2$-$x(OH)_3Cl$ nanoparticles with an optimal Ni/Co ratio suitable for use as cathodic materials [91], as a solvent and nitrogen source for preparing fluorescent carbon dots [92], and for the synthesis of titanomagnetite NPs with enzyme-like activity [93]. Finally, reline was also used very recently as a template to prepare polyacrylates/nanohydroxyapatite

scaffolds and polycrystalline sub-nanometrical chalcogen nanoparticles (SeTe) with high activity towards tumor cell lines [94].

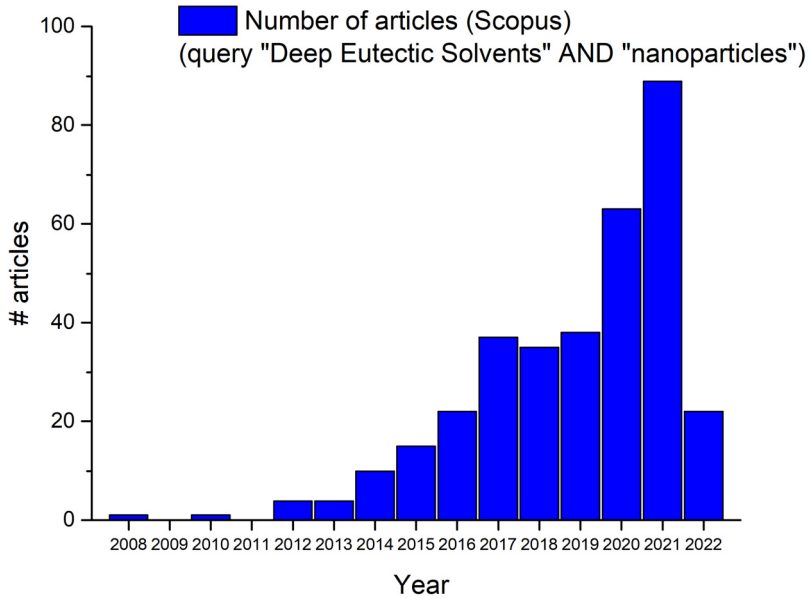

Figure 3. Number of published articles per year (2012–2022) corresponding to the Scopus query "Deep Eutectic Solvents AND nanoparticles" issued on 17 February 2022.

Regarding electrodeposition studies conducted in reline, several examples have been published in the last two years: for instance, water-soluble magnetic iron oxide nanoparticles were prepared at the anode during the electrolysis of reline using iron electrodes [95]; ruthenium nanoparticles were electrodeposited on stainless steel from a dichloride solution [96]; core–shell Pd-hydroxide NPs were obtained through the electrochemical oxidation of formic acid [97]; Zn/ZnO nanopowders were electrodeposited over Pt electrodes electrolyzing $ZnCl_2$ solutions [98]; copper nanoparticles were obtained from $CuCl_2 \cdot H_2O$ [99]. Some of the other "traditional" mixtures prepared in the first phase of DES development together with reline—namely, ethaline (choline chloride-ethylene glycol) and glyceline (choline chloride-glycerol)—have found a considerable number of applications recently. Ethaline was used as a medium for the electrodeposition of Ni nanoparticles. It was, suitable for the catalysis of methanol oxidation [100]; for the synthesis of NiS_2 nanospheres [101]; and, very interestingly, for the modification of Fe_2O_3 NPs to produce very specific electrochemical sensors—for H_2O_2, acetylcholine and the antibiotic dapsone [102]. Furthermore, ChCl:EG was used as a carrier and disperser for SiO_2@Fe_3O_4 (silica-coated magnetite) ferrofluids selective for Meloxicam [103], to electrodeposit Ni-Al nanocomposite coatings from $NiCl_2$ and aluminum dispersions [104], to synthesize platinum hollow-opened structures with enhanced performance in the electro-chemical oxidation of methanol [105], and as a solvent for assembling Ag nanoparticles onto copper substrates [106]. Glyceline was employed in the solvothermal preparation of functionalized metal-organic framework (MOF) nanoparticles containing zirconium [107], to immobilize Pd nanoparticles [108], and to deposit ZnO in situ on graphene sheets [109]. However, the real novelty of the last period consisted, as stated above, in the very large increase in the use of many new and alternative mixtures, often including biomolecules of natural origin. For instance, the excellent capabilities of glycerol as hydrogen bond donor in DES were further enhanced by the addition of malic acid and D-fructose in a 1:1:1: mole ratio (MaFruGly). MaFruGly was used to disperse Al_2O_3 into a nanofluid that is capable of extracting polyphenols and other bioactive compounds from olive oil pomaces and leaves [110]. Other examples of such biocompatible mixtures include choline chloride:glucose, which was used to prepare sodium hyaluronate/dopamine/AgNPs hydrogels [111]; ChCl:xylitol, which was employed to modify magnetic titania NPs with Fe_3O_4@TiO_2@DES [112]; and choline chloride:gluconic

acid DES, which was used to prepare a cobalt-DES precursor that was finally pyrolyzed into Co nanoparticles supported on nitrogen-doped porous carbon (Co@NPC). The latter acts as a bifunctional catalyst for water splitting (H_2 production) and glucose oxidation (GOR) in an electro-chemical cell [113]. Along the same line, carbon-doped copper oxide catalysts with a high selectivity in CO_2 electrochemical reduction were produced by the calcination of sugar-urea DES (glucose:urea and galactose:urea) containing copper salts [114]. Mixtures containing carboxylic acids have been described in several examples: ChCl + oxalic acid and malonic acid, together with urea, fructose, and ethylene glycol, were used to synthesize $MgFe_2O_4$ nanoparticles with a high sensitivity and selectivity towards nitrofenantoine and 4-nitrophenol [115]. Pd nanoparticles confined in nanocellulose with a high catalytic chemoselectivity and activity were prepared from choline chloride and oxalic acid dihydrate 1:1 [116] (this mixture was also employed as a medium to synthesize porous Fe_3O_4 nanosheets with high electrocatalytic performances starting from commercial powders) [117]. An example of a mixture of choline and inorganic salts is choline:Na_2SO_3 2:1, a "reductant" solvent where sulfur-functionalized graphene oxide NPs for Li-S batteries were synthesized using a chemical reduction/co-precipitation method [118].

A relevant portion of the recent studies on this topic has focused on magnetic nanoparticles containing Fe_3O_4 (or Fe_2O_3) and organic moieties or enzymes, which could be assembled in a few examples of DESs: acrylic acid-Fe_3O_4 composites were obtained from acrylic acid:menthol-type V DES used in the detection of pesticides [119], whereas macroporous polyacrylamide γ-maghemite composites were prepared in acetic acid:menthol [120]. Nano-Fe_3O_4 was prepared in NADES betaine-urea, coated with silicon, and successfully employed to immobilize β-glucosidase [121]. magnetite nanocubes with anticancer and photo-Fenton efficacy were synthesized in ChCl:citric acid by Sakthi Sri et al. [122]; poly glycerol@Fe_3O_4 nanoparticles (as HBD) were treated with choline chloride, giving a branched poly (DES)@ Fe_3O_4 fluid that was used as draw solute in forward osmosis [123], whereas DES coupled to Fe_3O_4-MUiO-66-NH_2 (a metal organic framework composed of zirconia clusters cross-linked by terephtalic acid) obtained from mixtures of quaternary ammonium salts different from choline, such as benzyltributylammonium chloride (BTBAC), benzyltributylammonium bromide (BTBAB), tetrabutylammonium chloride (TBAC) as HBA, and lactic or glycolic acid such as HBD was employed to adsorb pharmaceuticals and personal care products (PPCPs). The magnetic nanoparticles could be easily separated and recovered from the adsorbed species using a magnet [124]. Other examples of quaternary ammonium salts include TBAB (tetrabutylammonium bromide), which was combined with imidazole in a DES. The latter was employed as a solvent to immobilize Pd nanoparticles onto a covalent organic framework, finally resulting in a heterogeneous catalyst used for the phosphorylation of aryl bromides [125]. Furthermore, CTAB (cetyltrimethylammonium bromide), which combines with acetic acid in a 1:1 mass ratio to create a liquid mixture, was used for the formation of ceria nanoparticles with remarkable photocatalytic activity by Iqbal and coworkers [126,127]. Other sugar-based DESs similar to those cited above—namely, dl-menthol:oleyl alcohol 1:1.2—were employed to prepare an NDDES (nano dispersed DES) mixture containing boron nitride nanoparticles, with excellent properties as a heat-transfer nanofluid [128]. A comprehensive survey on the use of DES as a base fluid for heat-transfer nanofluids can be found in [29].

Table 1. Recent examples of "wet syntheses" in DES media.

Solvent	Reagents/Path	Product	References
ChCl:urea 1:2	Preparation of separate solutions of $HAuCl_4 \cdot 4\,H_2O$ (0.015 g) and L-ascorbic acid (LA, 0.05 g) in DES. Addition of LA solution to $HAuCl_4$ at 30 °C under magnetic stirring until the color changes from yellow to dark purple	**Au** nanoparticles Star, snowflake, or nano-thorn-shaped depending on water content	[49] (Figure 2)
	Direct electrodeposition on GC substrate in 19.3 mM H_2PtCl_6/DESs solution at 80 °C	Tetrahexahedral (THH) concave **Pt** NCs	[52]
		Triambic Icosahedral **Pt** NCs	[54]
	Mixing $CuCl_2 \cdot 2H_2O$ (5.0013 g, 0.0293 mol) and Cu powder (1.6935 g, 0.0265 mol) with DES, gentle stirring at 20 °C for 5 h, rinsing with diluted HCl	**CuCl** nanocrystal powder	[56]
	Addition of 2.2232 g of $CuCl_2$ $2H_2O$ and 1.3754 g of ascorbic acid to 14 mL DES in the presence of PVP, mild stirring at 25 °C for 1 h, rinsing with 50 mL HCl (0.1 M)	Spherical **CuCl** nanoparticles	[57]
	Addition of 2.164 g (8 mmol) $FeCl_3 \cdot 6H_2O$ and 1.194 g (6 mmol) $FeCl_2 \cdot 4H_2O$ to 15.585 g DES, stirring at ca. 600 rpm and 80 °C for 20 min, subsequent addition of 2.613 g (46.7 mmol) KOH, and stirring for another 1.5 h at 80 °C. Alternatively, see Figure 5 and last paragraph	Spherical, magnetic $\mathbf{Fe_3O_4}$ nanoparticles	[58]; Figure 5 and last paragraph
	Solvent: 35.70 g of DES (30 mL at 37 °C) and 6 mL of water. Dissolution of thioacetamide (TH, 12 mmol, 0.9134 g) mL into 12 mL of solvent and lead (IV) acetate (LAC, 12 mmol, 5.3206 g) into the remaining liquid, stirring of both solutions at 80 °C. Injection of TH into LAC changes the solution from pale yellow to opaque dark brown. Rinsing with water, followed by dialysis, centrifugation, and drying in furnace at $T \leq 80$ °C	Hyperbranched **PbS** Nano/microcrystals	[59]
	Heating of $NiCl_2 \cdot 6H_2O$ in DES (0.1 M solution) at 150 °C for 40 min; then addition of 10 mL of water and further stirring for 20 min, cooling in ice bath; drying of precursor overnight at 90 °C and further annealing in air (300 °C) for 4 h	Mesoporous **NiO**	[60]
	$NiCl_2 \cdot 6H_2O$ in DES ionothermal reactions at different temperatures and conditions	$\mathbf{Ni(NH_3)_6Cl_2}$, $\mathbf{NiCl_2}$ and nanoflower-like α-$\mathbf{Ni(OH)_2}$ and **NiO**	[61]
	Dissolution of 5.94 g of $Ni(H_2PO_2)_2 \cdot 6H_2O$ (0.02 mol) and 1.66 g of $NH_4H_2PO_2$ (0.02 mol) in 27.92 g (0.2 mol) of choline chloride and 24.02 g (0.4 mol) of urea, stirring at 323 K under N_2 for 30 min, reduction of product with H_2 at 673 K for 3 h	Ni_2P supported on amorphous/mesoporous $\mathbf{Ni_3(PO_4)_2}$-$\mathbf{Ni_2P_2O_7}$	[62]
	Emulsion of 2.25 g $SnCl_2 \cdot 2H_2O$ in 100 mL DES. Variable reaction times (1 to 60 min)	Nano-sized **SnO** particles (20–30 nm)	[63]
	Heating of 40 mL of 0.1 M $FeCl_3 \cdot 6H_2O$/DES solution at 200 °C, after 10 min. addition of 40 mL of water and further reaction for 10 min. Washing of precipitate with ethanol and dried at 80 °C overnight	$\mathbf{Fe_2O_3}$ nanospindles	[64]

Table 1. *Cont.*

Solvent	Reagents/Path	Product	References
ChCl:urea 1:2	Dissolving $CoCl_2 \cdot 6H_2O$ into ChCl to obtain a 0.1 M $CoCl_2$:ChCl solution, addition of 100 mL of water after heating for 40 min at different temperatures. Subsequent ice bath cooling, rinsing of product with water and methanol, and drying at 70 °C under vacuum	Mesoporous **Co_3O_4** sheets or nanoparticles	[65]
	DES solution of bulk ZnO. Precipitation with water (anti-solvent approach)	**ZnO** nanocrystals doped with Cu(II) ions	[67]
	Dissolution of $SnCl_2 \cdot 2H_2O$ in DES, stirring in pre-heated water bath (50, 80, 98 °C), precipitation with ethanol, and drying at 230 °C	**SnO_2** nanoparticles	[68]
	Mixing of y mmol $NiCl_2$ $6H_2O$ and 20-y mmol $CoCl_2$ $6H_2O$ (y = 0, 2.5, 5, 10) in 10 mL DES. Addition of 1 mmol SDS and 20 mL water, heating for 12 h at 100 °C, washing of precipitate with water and ethanol	**$NixCo_2$-$x(OH)_3Cl$**	[91]
	Stirring of 1.668 g (0.006 mol) $FeSO_4 \cdot 7H_2O$ and 0.584 g (0.010 mol) of KOH 0.408 g in DES for 30 min, addition of 0.408 g (0.0012 mol) tetrabutyl titanate (TBOT) and 0.420 g (0.008 mol) of KOH, stirring first at 80 °C (30 min) and then at 110 °C (4 h), washing of precipitate with water and ethanol	**$Fe_{2.5}Ti_{0.5}O_4$-DES** nanoparticles	[93]
ChCl:urea 1:2 ChCl:urea:water 1:2:10	Hydrothermal treatment of $Fe(NO_3)_3 \cdot 9H_2O$/DES mixtures (dry and hydrated DES) for 3–8 h at 90 °C before particles are dried at 60 °C from ethanol after dialysis	**FeO**	[88]
	Dissolution of $Ce(NO_3)_3 \cdot 6$ H_2O in DES and stirring at 250 rpm for 40 min, reaction in pressurized continuous microreactor at 100–160 °C, washing of the solid product with water and ethanol and drying at 80 °C	**CeO_2**	[89]
$(CH_3)NH_2$ HCl:urea 1:1.5	Mixture of Sn (0.119 g, 1.0 mmol), Se (0.211 g, 2.67 mmol), dimethylamine hydrochloride (0.58 g, 7.1 mmol), urea (0.64 g, 10.67 mmol), and 0.3 mL of $N_2H_4 \cdot H_2O$ (98%) (∼6.17 mmol), hydrothermal synthesis at 160 °C (3 h), rinsing with water	Silver and selenido-stannates **$[NH_4]_3AgSn_3Se_8$** **$[NH_4]_2Sn_4Se_9$** **$[NH_3C_2H_5]_2Sn_3Se_7$**	[82]
ChCl:oxalic acid 1:1	Dissolution of 30 mg of commercial Fe_3O_4 in 1 mL ChCl/OA DES at 50 °C by ultrasonic treatment, microwave heating for 10 s at 100 W, further thermal treatment at 300 °C for 2 h	**Fe_3O_4** nanosheets	[117]
	Addition of MgO and α-Fe_2O_3 to DES molar ratio 1:1 (0.5 wt% melt in the overall amount of metal oxides), stirring for 1 h, then calcination of melts at 500 °C for 1 h (5 °C min^{-1} heating rate)	**$MgFe_2O_4$** nanoparticles	[115]
ChCl:acrylic acid	Stirring of ChCl and MAA in the molar ratio 1:2 at 80 °C; mixing with a porogen (MeOH), initiator (AIBN), crosslinking agent (EGDMA), and template (levofloxacin); heating at 60 °C for 12 h; removal of template by Soxhlet extraction with methanol	Levofloxacin-imprinted **Pd** nanoparticles	[75]

Table 1. *Cont.*

Solvent	Reagents/Path	Product	References
ChCl:oxalic acid:water 1:1:1	Mixing of cellulose pulp (0.5 g) with DES (10 g) and water (10 g), heating at 110 °C for 2 h in a Teflon-lined reactor to obtain carboxylic cellulose (CNF). Addition of 10 mL of $PdCl_2$ (17.7 mg) in HCl and aqueous $NaBH_4$ (10 mg, 1 mL) to a diluted CNF suspension (20 mL, 0.4 wt%), reaction at 4 °C for 4 h, separation of Pd NPs by dialysis	**Pd** nanoparticles confined in nanocellulose	[116]
ChCl:ethylene glycol 1:2	Mixing of $NiSO_4 \cdot 6H_2O$ (0.1 M), $Na_2S_2O_3 \cdot 5H_2O$ (0.1 M), EDTA (0.06 M), and DES in a beaker at different temperatures (80 °C, 100 °C, 110 °C, 120 °C, 160 °C); stirring of the mixtures for 3 h; washing of the solids with water and ethanol; and drying at 60 °C	**NiS_2** nanospheres	[101]
	Dissolution of 4.0 mg of $Pt(acac)_2$, 40 mg PVP, and 25 mg of SDS in 8 mL DES; heating in oil bath at 130 °C for 2 h; washing of the black precipitate with ethanol	**Pt** hollow-opened structures	[105]
ChCl:glycerol 1:2	Hydrothermal heating of $ZrCl_4$, BDC (1,4 benzene dicarboxylate), H_2O, and DES at a molar ratio of 1:1:1:500 at 120 °C for 48 h; washing of the solid with water	Nanoparticles containing **$ZrCl_4$**	[107]
	Mixing 2.19 g of $Zn(CH_3COO)_2 \cdot 2H_2O$ and 0.2 g of graphene in 50 mL DES, precipitation with 0.8 g NaOH	**ZnO** in situ on graphene sheets	[109]
ChCl:$CaCl_2$ 1:2	CO_2 capture from air of $CaCl_2 \cdot 6H_2O$ and choline chloride DES at 50 °C under stirring at 400 rpm, formation of $CaCO_3$ sediment after 6 h, washing of the sediment with water, drying at 60 °C for 12 h, reuse of the filtrate for further CO_2 capture	**$CaCO_3$** NPs	[78]
ChCl:glucose/fructose/ sucrose/maltose/ raffinose	Liquid-phase exfoliation of MoS_2 in glucose, fructose, sucrose, raffinose, maltose, choline chloride, and water DES at various ratios (5 mg MoS_2 per mL of DES); separation of exfoliated material in ethanol/water	**MoS_2** nanosheets	[77]
CHCl:glucose	DASH: Dopamine hydrochloride (DA), N-Hydroxysuccinimide (NHS), 1-ethyl-3-(3-(dimethylamino)propyl) carbodiimide (EDC), sodium hyaluronate (SH) in 2-(N-morpholino) ethanesulfonic acid-buffered solution (MES buffer). Addition of $AgNO_3$ to DES-DASH 4:175 mixture	**Na hyaluronate/dopamine/Ag NPs** hydrogels	[111]
ChCl:xylitol 1:1	Mixing 0.2 g Fe_3O_4@TiO_2 nanoparticles and 3.0 mL [ChCl][Xyl] by ultrasonication for 2 h, separation by external magnet, rinsing with water	**Fe_3O_4@TiO_2@DES**	[112]
ChCl:gluconic acid	Mixing 2 g choline chloride, 4 g urea, and 0.4 g $Co(NO_3)_2 \cdot 6H_2O$ in 5.62 mL of 50% gluconic acid solution; calcination in N_2 at 700–900 °C after freeze-drying	**Co@NPC**	[113]

Table 1. *Cont.*

Solvent	Reagents/Path	Product	References
CHCl:citric acid 2:1	Addition of 3.9813 g $FeCl_2$ $4H_2O$ (20 mM) and 8.1091 g of $FeCl_3.6H_2O$ (30 mM) at the molar ratio 1:1.5 to DES, stirring at 80 °C (600 rpm) for 20 min, addition of 40 g (712.94 mM) KOH, stirring for another 1 h, washing with ethanol and water	**Fe_3O_4** nanocubes	[122]
Betaine-urea 1:2	DES: betaine (2.343 g) and urea (2.4 g), heating for 15 min at 125 °C, addition of 1.5 mL water, dissolution of 0.111 g $FeSO_4{\cdot}7H_2O$ (0.4 mmol) and 0.216 g $FeCl_3{\cdot}6H_2O$ (0.8 mmol) in DES at RT under stirring (10 min), precipitation by the addition of 0.2 g of KOH (3.5 mmol), separation with external magnet, and washing with water	Nano-**Fe_3O_4** Nano-**Fe_3O_4**@SiO_2–NH_2	[121]
BTAB/BTBAC/ TBAC:lactic acid	[BTBAC][Lac]-DES: Mixing 3.12 g BTBAC and 1.80 g Lac at a molar ratio 1:2 under heating at 80 °C in oil bath for 1 h. Addition of 2.0 mL DES to a phosphate buffer (20 mM, pH = 7.0) containing 0.24 g of NHS and 0.16 g of EDC·HCl to activate the carboxyl group of DES; subsequently, the addition of 0.20 g MUiO-66-NH_2, stirring for 12 h, washing of particles with water, and freeze-drying	**Fe_3O_4**-MUiO-66-NH_2	[124]
TBAB:imidazole	Condensation of TFPT (main building block) and hydrazine (comonomer) in BuN_4Im/Br at 90 °C for 12 h, subsequent impregnation with $Pd(oAC)_2$ under reflux	**Pd@MOF**	[125]
CTAB:acetic acid 1:1	Mixing cetyltrimethylammonium and acetic acid at 70 °C for 3 h. Addition of 1 g ammonium cerium (IV) nitrate to 0.5 g of DES and hydrothermal treatment of the solution at 130 °C for 7 h. For N-doping, a urea solution (10 g/30 mL of water) is added, followed by the separation of particles by centrifugation and washing with ethanol and acetone	Plain and N-doped **CeO_2**	[126,127]
dl-menthol:oleyl alcohol 1:1.2	Mixing 1 mol D,L-menthol and oleyl alcohol at 343.15 K under stirring for 12–24 h. Addition of h-BN nanoparticles at different weight percentages, shaking, and sonication for 2 h	**BN** nanoparticle nanofluid	[128]
Acetic acid:menthol 1:2 pyruvic acid:menthol 1:1 lactic acid:menthol 1:2 lauric acid:menthol 2:1	Mixing of D,L-menthol with PA, AA, LacA, or LauA at 50 °C for 15 min before drying under vacuum (10^{-1} Pa). Preparation of high-internal-phase emulsions (HIPEs) by dropping DES into a continuous phase of AAm:BAAm (acrylamide:N,N′-Methylenebis(acrylmide), polymerization with potassium persulfate (KPS), and coating with γ-Fe_2O_3	Polyacrylamide γ-maghemite composites	[120]
Acrylic acid:mentho 1:2	Mixing AA and menthol at 70 °C in a water bath for 5 min, polymerization of DES via a thermal frontal method usingFe_3O_4 NPs-AA as a cross-linker and thermal initiator into a magnetic poly (AA-menthol DES) hydrogel	**Acrylic acid**:**Fe_3O_4** composites	[119]

Table 1. *Cont.*

Solvent	Reagents/Path	Product	References
Choline:Na_2SO_3 2:1	Heating of 7.0 g of choline chloride and ~4.0 g NaS_2O_3 in 2:1 molar ratio at 40 °C for 3 h. Addition of 16 mL DES to a GO solution in the presence of hydrazine as a reducing agent, co-precipitation of reduced GO and sulfur	Sulfur-functionalized **graphene oxide** NPs	[118]
Dimethylammonium nitrate:triethylene/ ethylene glycol, or glycerol 1:1	HBA: Addition of 119.4 mL of 5.0 N HNO_3 solution (0.597 mol) to aqueous dimethylamine (40 wt% in H_2O, 0.597 mol). HBD: triethylene glycol, ethylene glycol, or glycerol. Addition of $HAuCl_4$ or $AgNO_3$ and oleylamine (OAm) (reducing agent) in each DES under stirring (150 rpm); heating at different temperatures (12 h at 60 °C for Ag, 19 min. 140–170 °C for Au)	**Ag** or **Au** colloidal nanocrystals	[81]

5. Lewis Acid DES (LADES)

A smaller number of studies were dedicated to DES without quaternary ammonium salts, containing metal salts (often hydrated) such as HBA and hydrogen bond donors such as urea or acetamide. This family of DES is known as LADES (Lewis Acid DES)) [129], compared to the more common "BADES" (with Brønsted acids, such as choline chloride + oxalic acid). According to the Abbot classification, LADES belong to Type I, II, or IV DES (such as, for instance, ChCl:2$ZnCl_2$, ChCl:2$CrCl_3$·6H_2O, $ZnCl_2$:urea 1:3.5 (or:4) melts), as do several amide-nitrate eutectics [130] (such as $LiNO_3$:acetamide 22:78 eutectic, which was recently described as a valuable medium for electrochemical capacitors [131]) and the DES mixture already described (silver triflate:acetamide [79]), while Type III DES can form only BADES. The existence of these non-conventional melts was quite recently discussed regarding the preparation or modification of inorganic nanoparticles. These DES include chloride salts, which have been employed in three different preparations of titania-based nanomaterials: the nano-photocatalyst n-TiO_2-P25@TDI@DES, which is highly recyclable and selective, was obtained by combining TiO_2-P25 powder (70% anatase, 30% rutile) with a $ZnCl_2$:urea 1:4 mixture using 2,4-toluene diisocyanate (TDI) as a bifunctional covalent linker. The nanocatalyst was employed successfully in the oxidation of benzyl alcohols to aldehydes and sulfides to sulfoxides [132,133]; the synergy between LADES and NPs was also exploited in the coupling between "Hierarchical TiO_2" (H-TiO_2) microspheres and $FeCl_2$/$CuCl_2$ urea in 1:4 mixtures to increase the reaction yields in the preparation of pyrrolidyn-2-one heterocycles [134] and by grafting the $ZnCl_2$:urea 1:4 mixture onto magnetic ferrite nanoparticles to generate a DES@MNP homogeneous catalyst (which was found to be "magnetically recyclable" at the end of one-pot multicomponent syntheses [135]). Coming back to the synthesis of the nanoparticles themselves, some lanthanide-based type IV DES (Ln-DES) containing hydrated nitrates were prepared [136]. These mixtures show unusually low viscosity and surface tensions and the presence of fluxional oligomeric polyanions and polycations, and were employed as reaction media in the combustion synthesis of oxides; more recently, actinide-based type IV DES (An-DES) were obtained by mixing uranyl nitrate hexahydrate $UO_2(NO_3)_2$·6H_2O (UNH) with urea in different ratios (Figure 4), finding 0.2:0.8 to be the optimal UNH:urea mole fraction, with a quite low eutectic temperature of −5.2 °C. This liquid was employed to prepare UO_2 nanoparticles through an optimized electrosynthesis path [137]. Some examples of reactions in LADES are given in Table 2.

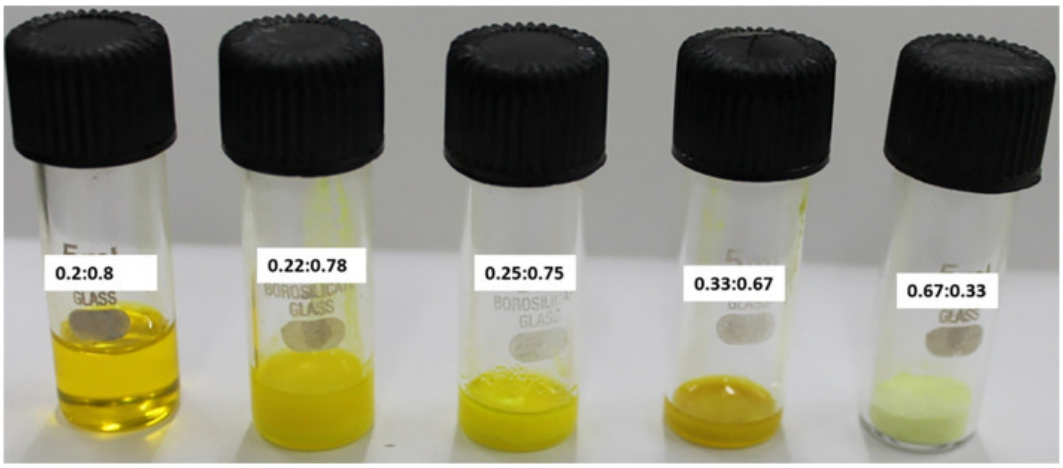

Figure 4. Examples of liquid mixtures of $UO_2(NO_3)_2 \cdot 6H_2O$ + urea DES, reproduced with permission from ref. [137]. Copyright 2021 Elsevier.

Aside from metal nanoparticles, DES are finding wide application nowadays in the production of lignin and cellulose nanoparticles. A basic knowledge of this widely investigated topic, though not closely related to the focus of this article, can help in showing further examples of eutectic mixtures, particularly the newest natural biocompatible ones, that could somehow be adapted and employed for the synthesis of systems containing metals. Among the most recent examples worth mentioning are mixtures of choline chloride:glycerol (or ethylene glycol) with $AlCl_3$ [138]; choline chloride with ethanolamine or polyvinyl alcohol [139,140]; and choline chloride coupled with carboxylic acids (such as oxalic or lactic acid [141]) or with inorganic salts (Gly-K_2CO_3) [142]), DES lactic acid-betaine [142], and menthol-based melts (e.g., menthol:dodecanoic acid [143]).

Table 2. Examples of reactions in type IV DES (LADES).

Solvent	Reagents/Path	Product	References
Lanthanide nitrate hydrate:urea 1:3.5	Mixing of cerium (III) nitrate hexahydrate, neodymium(III) nitrate hexahydrate, or praseodymium(III) nitrate with urea at various ratios; preferred ratio is 1:3.5	**Lanthanide oxides CeO_2, Pr_6O_{11}, NdO_3 + mixed carbonates**	[140]
$UNH(UO_2(NO_3)_2 \cdot 6H_2O)$:urea at various ratios	Mixing of UNH:urea at ratios 0.9:0.1, 0.8:0.2, 0.75:0.25, 0.6:0.4, 0.5:0.5, 0.33:0.67, 0.2:0.8, 0.1:0.9. Melting point of −5.2 °C for the 0.8:0.2 mixture	**UO_2** NPs	[141]
$ZnCl_2$:urea 1:4	DES: Urea (20.0 mmol, 1.200 g) and zinc chloride (5.0 mmol, 0.680 g). Covalent bonding of TiO_2 to DES through 2,4-toluene diisocyanate (TDI). Dispersion of 0.5 g of TiO_2@TDI NPs in DES with stirring at 100 °C for 18 h; washing with ethanol and drying at 60 °C under reduced pressure for 6 h	**Ti@DES** nanocatalyst	[136,137]

6. A Prototypical Synthesis

In order to show the potential and ease of obtaining inorganic nanoparticles in DES, we show a prototypical NP synthesis carried out in DES in the following paragraph. In particular, the co-precipitation of the mixed salt Fe_3O_4 (structurally $FeO \cdot Fe_2O_3$) from Fe^{2+} and Fe^{3+} soluble salt solutions in Choline-Urea 1:2 DES (reline) upon the addition of sodium

hydroxide will be shown. The procedure was first reported in [56] and was modified for this test preparation according to the following protocol:

(a) Preparation of DES

Totals of 11.108 g of dry choline chloride (MM = 139.62, 80 mmoles) and 9.610 g of urea (MM = 60.06, 160 mmoles) were weighted separately and kept in closed containers. The two solids were then mixed in a sealable vial at room temperature. Quite rapidly, the two solids when put in contact formed a sluggish agglomerate that became more fluid and transparent with gentle heating (35–40 °C); see Figure 3, first panel.

(b) Preparation of the solution

Totals of 0.130 g of $FeCl_3$ (0.8 mmoles) and 0.167 g of $FeSO_4 \cdot 7\ H_2O$ (0.6 mmol) were weighed and added to 1.559 g of the prepared DES in a 25 mL beaker. The dissolution was accelerated by heating the mixture at 80 °C, resulting in an orange transparent liquid; see Figure 5, second panel. The total amount of water introduced into the system (by counting the hydration water molecules coming from $FeSO_4$ and estimating those coming from the average absorbed water content of the two DES precursors (ChCl and urea) by weighing samples of the powders before and after a three day-long drying treatment at 50 °C in an oven) was well below the upper limit (10 moles of water per mole of DES), as identified in the neutron diffraction study by Hammond et al. [48], beyond which the microscopic features of pure reline were lost and the system turned into a three-component HBA:HBD:water mixture.

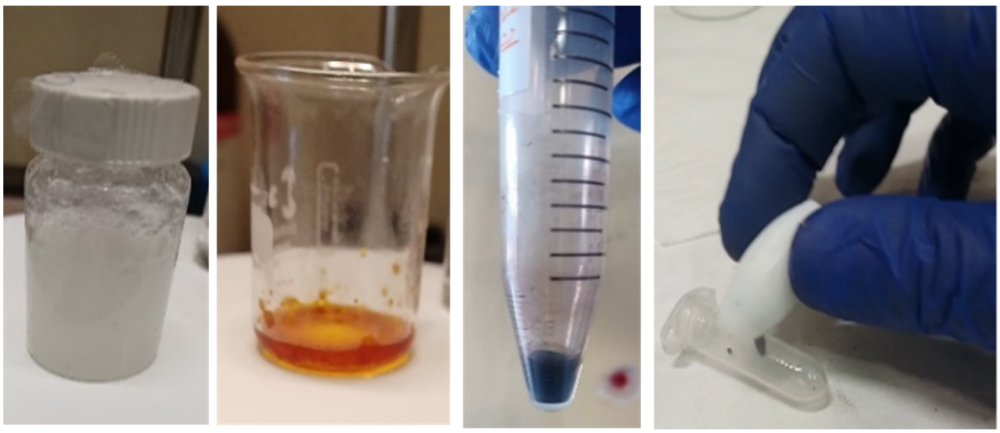

Figure 5. Demonstrative synthesis of magnetite nanoparticles. From left to right: Choline-Urea 1:2 DES forming at 35 °C; $FeCl_3$ and $FeSO_4$ salts dissolved in Choline-Urea 1:2 at 80 °C; Fe_3O_4 precipitate is formed on the addition of solid NaOH; after washing with water and drying at 40 °C, a magnetic solid bead is obtained.

(c) Precipitation

A total of 0.187 g of NaOH (previously powdered in an agate mortar, 46.7 mmol) was added to the solution at 80 °C under magnetic stirring (600 rpm). After 20 min, a black precipitate formed; see Figure 5, third panel. The precipitate was washed with 20 mL of distilled water four times and centrifuged for 5 min at 3000 rpm after each rinse cycle. The excess of DES crystallized upon contact with cold water but was gradually solubilized. The final pH after the washing was around 7, signaling that the excess amounts of NaOH and urea had been washed out.

(d) Drying

The washed precipitate was collected from the vial, dried at 40 °C and finally rolled into a bead. The bead was put into an Eppendorf tube, and its ferromagnetism was qualitatively tested with a magnetic stir bar (Figure 5, fourth panel)

7. Conclusions

In this small contribution, an overview of the newest and most important features of Deep Eutectic Solvents in the field of nanoparticle synthesis is given. We demonstrate that these mostly benign and inexpensive reaction media can be employed in different types of wet synthesis, as well as in electrochemical preparations. The reported reaction schemes are often straightforward and do not require complicated set-ups or equipment. The inherent inhomogeneity of the liquid mixtures exerts a direct templating effect without the use of any additives, and nanosystems of different topologies/shapes can be obtained. This field is being actively developed, as seen by the ever-increasing number of articles published, and its huge potential will surely continue to be explored, in search of new materials with beneficial technological properties.

Author Contributions: Conceptualization: L.G. and M.C.; writing—original draft preparation, L.G.; writing—review and editing: L.G., E.M.B. and M.B.; supervision, M.C.; project administration, M.C.; funding acquisition, M.C. and P.T.; investigation, L.G. and D.T.D. All authors have read and agreed to the published version of the manuscript.

Funding: This research received no external funding.

Conflicts of Interest: The authors declare no conflict of interest.

References

1. Ealia, S.A.M.; Saravanakumar, M.P. A Review on the Classification, Characterisation, Synthesis of Nanoparticles and Their Application. *IOP Conf. Ser. Mater. Sci. Eng.* **2017**, *263*, 032019. [CrossRef]
2. Jeevanandam, J.; Barhoum, A.; Chan, Y.S.; Dufresne, A.; Danquah, M.K. Review on Nanoparticles and Nanostructured Materials: History, Sources, Toxicity and Regulations. *Beilstein J. Nanotechnol.* **2018**, *9*, 1050–1074. [CrossRef] [PubMed]
3. Wang, Z.; Wang, X.; Zhao, N.; He, J.; Wang, S.; Wu, G.; Cheng, Y. The Desirable Dielectric Properties and High Thermal Conductivity of Epoxy Composites with the Cobweb-Structured SiCnw–SiO_2–NH_2 Hybrids. *J. Mater. Sci. Mater. Electron.* **2021**, *32*, 20973–20984. [CrossRef]
4. Wang, Z.; Meng, G.; Wang, L.; Tian, L.; Chen, S.; Wu, G.; Kong, B.; Cheng, Y. Simultaneously Enhanced Dielectric Properties and Through-Plane Thermal Conductivity of Epoxy Composites with Alumina and Boron Nitride Nanosheets. *Sci. Rep.* **2021**, *11*, 2495. [CrossRef] [PubMed]
5. Carbone, M.; Briancesco, R.; Bonadonna, L. Antimicrobial Power of Cu/Zn Mixed Oxide Nanoparticles to Escherichia Coli. *Environ. Nanotechnol. Monit. Manag.* **2017**, *7*, 97–102. [CrossRef]
6. Carbone, M. Cu Zn Co Nanosized Mixed Oxides Prepared from Hydroxycarbonate Precursors. *J. Alloys Compd.* **2016**, *688*, 202–209. [CrossRef]
7. Carbone, M. CQDs@NiO: An Efficient Tool for CH4 Sensing. *Appl. Sci.* **2020**, *10*, 6251. [CrossRef]
8. Carbone, M.; Tagliatesta, P. NiO Grained-Flowers and Nanoparticles for Ethanol Sensing. *Materials* **2020**, *13*, 1880. [CrossRef]
9. Carbone, M.; Aneggi, E.; Figueredo, F.; Susmel, S. NiO-Nanoflowers Decorating a Plastic Electrode for the Non-Enzymatic Amperometric Detection of H_2O_2 in Milk: Old Issue, New Challenge. *Food Control* **2022**, *132*, 108549. [CrossRef]
10. Carbone, M.; Nesticò, A.; Bellucci, N.; Micheli, L.; Palleschi, G. Enhanced Performances of Sensors Based on Screen Printed Electrodes Modified with Nanosized NiO Particles. *Electrochim. Acta* **2017**, *246*, 580–587. [CrossRef]
11. Carbone, M.; Missori, M.; Micheli, L.; Tagliatesta, P.; Bauer, E.M. NiO Pseudocapacitance and Optical Properties: Does the Shape Win? *Materials* **2020**, *13*, 1417. [CrossRef] [PubMed]
12. Carbone, M.; Maria Bauer, E.; Micheli, L.; Missori, M. NiO Morphology Dependent Optical and Electrochemical Properties. *Colloids Surf. A Physicochem. Eng. Asp.* **2017**, *532*, 178–182. [CrossRef]
13. Tan, S.; Ebrahimi, A.; Liu, X.; Langrish, T. Role of Templating Agents in the Spray Drying and Postcrystallization of Lactose for the Production of Highly Porous Powders. *Dry. Technol.* **2018**, *36*, 1882–1891. [CrossRef]
14. Li, Y.; Khuu, N.; Prince, E.; Alizadehgiashi, M.; Galati, E.; Lavrentovich, O.D.; Kumacheva, E. Nanoparticle-Laden Droplets of Liquid Crystals: Interactive Morphogenesis and Dynamic Assembly. *Sci. Adv.* **2019**, *5*, eaav1035. [CrossRef] [PubMed]
15. Holmberg, K. Surfactant-Templated Nanomaterials Synthesis. *J. Colloid Interface Sci.* **2004**, *274*, 355–364. [CrossRef]
16. Xie, H.; Gu, Y.; Ploehn, H.J. Dendrimer-Mediated Synthesis of Platinum Nanoparticles: New Insights from Dialysis and Atomic Force Microscopy Measurements. *Nanotechnology* **2005**, *16*, S492–S501. [CrossRef] [PubMed]
17. Wagle, D.V.; Zhao, H.; Baker, G.A. Deep Eutectic Solvents: Sustainable Media for Nanoscale and Functional Materials. *Acc. Chem. Res.* **2014**, *47*, 2299–2308. [CrossRef]
18. Hansen, B.B.; Spittle, S.; Chen, B.; Poe, D.; Zhang, Y.; Klein, J.M.; Horton, A.; Adhikari, L.; Zelovich, T.; Doherty, B.W.; et al. Deep Eutectic Solvents: A Review of Fundamentals and Applications. *Chem. Rev.* **2021**, *121*, 1232–1285. [CrossRef]
19. Abo-Hamad, A.; Hayyan, M.; AlSaadi, M.A.; Hashim, M.A. Potential Applications of Deep Eutectic Solvents in Nanotechnology. *Chem. Eng. J.* **2015**, *273*, 551–567. [CrossRef]

20. Smith, E.L.; Abbott, A.P.; Ryder, K.S. Deep Eutectic Solvents (DESs) and Their Applications. *Chem. Rev.* **2014**, *114*, 11060–11082. [CrossRef]
21. Abbott, A.P.; Capper, G.; Davies, D.L.; Rasheed, R.K.; Tambyrajah, V. Novel Solvent Properties of Choline Chloride/Urea Mixtures. *Chem. Commun.* **2003**, *39*, 70–71. [CrossRef] [PubMed]
22. Meng, X.; Ballerat-Busserolles, K.; Husson, P.; Andanson, J.-M. Impact of Water on the Melting Temperature of Urea + Choline Chloride Deep Eutectic Solvent. *New J. Chem.* **2016**, *40*, 4492–4499. [CrossRef]
23. Arkawaz, A.F.; Abdullah, B.A.; Mustafa Ha, S. Physical, Thermal and Structural Properties of 1 Choline Chloride: 2 Urea Based Ionic Liquids. *Singap. J. Sci. Res.* **2020**, *10*, 417–424. [CrossRef]
24. Lapeña, D.; Bergua, F.; Lomba, L.; Giner, B.; Lafuente, C. A Comprehensive Study of the Thermophysical Properties of Reline and Hydrated Reline. *J. Mol. Liq.* **2020**, *303*, 112679. [CrossRef]
25. Ribeiro, B.D.; Florindo, C.; Iff, L.C.; Coelho, M.A.Z.; Marrucho, I.M. Menthol-Based Eutectic Mixtures: Hydrophobic Low Viscosity Solvents. *ACS Sustain. Chem. Eng.* **2015**, *3*, 2469–2477. [CrossRef]
26. Liu, Y.; Friesen, J.B.; McAlpine, J.B.; Lankin, D.C.; Chen, S.-N.; Pauli, G.F. Natural Deep Eutectic Solvents: Properties, Applications, and Perspectives. *J. Nat. Prod.* **2018**, *81*, 679–690. [CrossRef]
27. Paiva, A.; Craveiro, R.; Aroso, I.; Martins, M.; Reis, R.L.; Duarte, A.R.C. Natural Deep Eutectic Solvents–Solvents for the 21st Century. *ACS Sustain. Chem. Eng.* **2014**, *2*, 1063–1071. [CrossRef]
28. Gontrani, L.; Plechkova, N.V.; Bonomo, M. In-Depth Physico-Chemical and Structural Investigation of a Dicarboxylic Acid/Choline Chloride Natural Deep Eutectic Solvent (NADES): A Spotlight on the Importance of a Rigorous Preparation Procedure. *ACS Sustain. Chem. Eng.* **2019**, *7*, 12536–12543. [CrossRef]
29. Jafari, K.; Fatemi, M.H.; Estellé, P. Deep Eutectic Solvents (DESs): A Short Overview of the Thermophysical Properties and Current Use as Base Fluid for Heat Transfer Nanofluids. *J. Mol. Liq.* **2021**, *321*, 114752. [CrossRef]
30. Kanzaki, R.; Uchida, K.; Song, X.; Umebayashi, Y.; Ishiguro, S. Acidity and Basicity of Aqueous Mixtures of a Protic Ionic Liquid, Ethylammonium Nitrate. *Anal. Sci.* **2008**, *24*, 1347–1349. [CrossRef]
31. Mariani, A.; Bonomo, M.; Gao, X.; Centrella, B.; Nucara, A.; Buscaino, R.; Barge, A.; Barbero, N.; Gontrani, L.; Passerini, S. The Unseen Evidence of Reduced Ionicity: The Elephant in (the) Room Temperature Ionic Liquids. *J. Mol. Liq.* **2021**, *324*, 115069. [CrossRef]
32. Abbott, A.P.; Capper, G.; Davies, D.L.; McKenzie, K.J.; Obi, S.U. Solubility of Metal Oxides in Deep Eutectic Solvents Based on Choline Chloride. *J. Chem. Eng. Data* **2006**, *51*, 1280–1282. [CrossRef]
33. Carriazo, D.; Gutiérrez, M.C.; Ferrer, M.L.; del Monte, F. Resorcinol-Based Deep Eutectic Solvents as Both Carbonaceous Precursors and Templating Agents in the Synthesis of Hierarchical Porous Carbon Monoliths. *Chem. Mater.* **2010**, *22*, 6146–6152. [CrossRef]
34. Raghuwanshi, V.S.; Ochmann, M.; Hoell, A.; Polzer, F.; Rademann, K. Deep Eutectic Solvents for the Self-Assembly of Gold Nanoparticles: A SAXS, UV–Vis, and TEM Investigation. *Langmuir* **2014**, *30*, 6038–6046. [CrossRef] [PubMed]
35. Alizadeh, V.; Geller, D.; Malberg, F.; Sánchez, P.B.; Padua, A.; Kirchner, B. Strong Microheterogeneity in Novel Deep Eutectic Solvents. *ChemPhysChem* **2019**, *20*, 1786–1792. [CrossRef] [PubMed]
36. Parnham, E.R.; Drylie, E.A.; Wheatley, P.S.; Slawin, A.M.Z.; Morris, R.E. Ionothermal Materials Synthesis Using Unstable Deep-Eutectic Solvents as Template-Delivery Agents. *Angew. Chem.* **2006**, *118*, 5084–5088. [CrossRef]
37. Chen, J.; Ali, M.C.; Liu, R.; Munyemana, J.C.; Li, Z.; Zhai, H.; Qiu, H. Basic Deep Eutectic Solvents as Reactant, Template and Solvents for Ultra-Fast Preparation of Transition Metal Oxide Nanomaterials. *Chin. Chem. Lett.* **2020**, *31*, 1584–1587. [CrossRef]
38. Hammond, O.S.; Bowron, D.T.; Edler, K.J. Liquid Structure of the Choline Chloride-Urea Deep Eutectic Solvent (Reline) from Neutron Diffraction and Atomistic Modelling. *Green Chem.* **2016**, *18*, 2736–2744. [CrossRef]
39. McDonald, S.; Murphy, T.; Imberti, S.; Warr, G.G.; Atkin, R. Amphiphilically Nanostructured Deep Eutectic Solvents. *J. Phys. Chem. Lett.* **2018**, *9*, 3922–3927. [CrossRef]
40. Cui, Y.; Rushing, J.C.; Seifert, S.; Bedford, N.M.; Kuroda, D.G. Molecularly Heterogeneous Structure of a Nonionic Deep Eutectic Solvent Composed of *N*-Methylacetamide and Lauric Acid. *J. Phys. Chem. B* **2019**, *123*, 3984–3993. [CrossRef]
41. Sahu, S.; Banu, S.; Sahu, A.K.; Phani Kumar, B.V.N.; Mishra, A.K. Molecular-Level Insights into Inherent Heterogeneity of Maline Deep Eutectic System. *J. Mol. Liq.* **2022**, *350*, 118478. [CrossRef]
42. Karimi, M.; Rastegar Ramsheh, M.; Mohammad Ahmadi, S.; Reza Madani, M. One-Step and Low-Temperature Synthesis of Monetite Nanoparticles in an All-in-One System (Reactant, Solvent, and Template) Based on Calcium Chloride-Choline Chloride Deep Eutectic Medium. *Ceram. Int.* **2017**, *43*, 2046–2050. [CrossRef]
43. Jhang, P.-C.; Chuang, N.-T.; Wang, S.-L. Layered Zinc Phosphates with Photoluminescence and Photochromism: Chemistry in Deep Eutectic Solvents. *Angew. Chem.* **2010**, *122*, 4296–4300. [CrossRef]
44. Di Carmine, G.; Abbott, A.P.; D'Agostino, C. Deep eutectic solvents: Alternative reaction media for organic oxidation reactions. *React. Chem. Eng.* **2021**, *6*, 582–598. [CrossRef]
45. Wei, X.; Chen, J.; Ali, M.C.; Munyemana, J.C.; Qiu, H. Cadmium Cobaltite Nanosheets Synthesized in Basic Deep Eutectic Solvents with Oxidase-like, Peroxidase-like, and Catalase-like Activities and Application in the Colorimetric Assay of Glucose. *Microchim. Acta* **2020**, *187*, 314. [CrossRef] [PubMed]

46. Bonomo, M.; Gontrani, L.; Capocefalo, A.; Sarra, A.; Nucara, A.; Carbone, M.; Postorino, P.; Dini, D. A Combined Electrochemical, Infrared and EDXD Tool to Disclose Deep Eutectic Solvents Formation When One Precursor Is Liquid: Glyceline as Case Study. *J. Mol. Liq.* **2020**, *319*, 114292. [CrossRef]
47. Hammond, O.S.; Li, H.; Westermann, C.; Al-Murshedi, A.Y.M.; Endres, F.; Abbott, A.P.; Warr, G.G.; Edler, K.J.; Atkin, R. Nanostructure of the Deep Eutectic Solvent/Platinum Electrode Interface as a Function of Potential and Water Content. *Nanoscale Horiz.* **2019**, *4*, 158–168. [CrossRef]
48. Hammond, O.S.; Bowron, D.T.; Edler, K.J. The Effect of Water upon Deep Eutectic Solvent Nanostructure: An Unusual Transition from Ionic Mixture to Aqueous Solution. *Angew. Chem.* **2017**, *129*, 9914–9917. [CrossRef]
49. Liao, H.-G.; Jiang, Y.-X.; Zhou, Z.-Y.; Chen, S.-P.; Sun, S.-G. Shape-Controlled Synthesis of Gold Nanoparticles in Deep Eutectic Solvents for Studies of Structure-Functionality Relationships in Electrocatalysis. *Angew. Chem. Int. Ed.* **2008**, *47*, 9100–9103. [CrossRef]
50. Sales, V.; Paternoster, C.; Mantovani, D.; Kolliopoulos, G. Fe–Mn Alloys Electroforming Process Using Choline Chloride Based Deep Eutectic Solvents. *Mater. Proc.* **2021**, *5*, 40. [CrossRef]
51. Maciej, A.; Łatanik, N.; Sowa, M.; Matuła, I.; Simka, W. Electrodeposition of Copper and Brass Coatings with Olive-Like Structure. *Materials* **2021**, *14*, 1762. [CrossRef] [PubMed]
52. Wei, L.; Fan, Y.-J.; Tian, N.; Zhou, Z.-Y.; Zhao, X.-Q.; Mao, B.-W.; Sun, S.-G. Electrochemically Shape-Controlled Synthesis in Deep Eutectic Solvents—A New Route to Prepare Pt Nanocrystals Enclosed by High-Index Facets with High Catalytic Activity. *J. Phys. Chem. C* **2012**, *116*, 2040–2044. [CrossRef]
53. Hammons, J.A.; Muselle, T.; Ustarroz, J.; Tzedaki, M.; Raes, M.; Hubin, A.; Terryn, H. Stability, Assembly, and Particle/Solvent Interactions of Pd Nanoparticles Electrodeposited from a Deep Eutectic Solvent. *J. Phys. Chem. C* **2013**, *117*, 14381–14389. [CrossRef]
54. Wei, L.; Zhou, Z.-Y.; Chen, S.-P.; Xu, C.-D.; Su, D.; Schuster, M.E.; Sun, S.-G. Electrochemically Shape-Controlled Synthesis in Deep Eutectic Solvents: Triambic Icosahedral Platinum Nanocrystals with High-Index Facets and Their Enhanced Catalytic Activity. *Chem. Commun.* **2013**, *49*, 11152. [CrossRef] [PubMed]
55. Das, N.; Kumar, A.; Rayavarapu, R.G. The Role of Deep Eutectic Solvents and Carrageenan in Synthesizing Biocompatible Anisotropic Metal Nanoparticles. *Beilstein J. Nanotechnol.* **2021**, *12*, 924–938. [CrossRef]
56. Zhang, F.; Lai, J.; Huang, Y.; Li, F.; Luo, G.; Chu, G. A Green Method for Preparing CuCl Nanocrystal in Deep Eutectic Solvent. *Aust. J. Chem.* **2013**, *66*, 237. [CrossRef]
57. Huang, Y.; Shen, F.; La, J.; Luo, G.; Lai, J.; Liu, C.; Chu, G. Synthesis and Characterization of CuCl Nanoparticles in Deep Eutectic Solvents. *Part. Sci. Technol.* **2013**, *31*, 81–84. [CrossRef]
58. Chen, F.; Xie, S.; Zhang, J.; Liu, R. Synthesis of Spherical Fe_3O_4 Magnetic Nanoparticles by Co-Precipitation in Choline Chloride/Urea Deep Eutectic Solvent. *Mater. Lett.* **2013**, *112*, 177–179. [CrossRef]
59. Querejeta-Fernández, A.; Hernández-Garrido, J.C.; Yang, H.; Zhou, Y.; Varela, A.; Parras, M.; Calvino-Gámez, J.J.; González-Calbet, J.M.; Green, P.F.; Kotov, N.A. Unknown Aspects of Self-Assembly of PbS Microscale Superstructures. *ACS Nano* **2012**, *6*, 3800–3812. [CrossRef]
60. Gu, C.D.; Huang, M.L.; Ge, X.; Zheng, H.; Wang, X.L.; Tu, J.P. NiO Electrode for Methanol Electro-Oxidation: Mesoporous vs. Nanoparticulate. *Int. J. Hydrogen Energy* **2014**, *39*, 10892–10901. [CrossRef]
61. Ge, X.; Gu, C.D.; Lu, Y.; Wang, X.L.; Tu, J.P. A Versatile Protocol for the Ionothermal Synthesis of Nanostructured Nickel Compounds as Energy Storage Materials from a Choline Chloride-Based Ionic Liquid. *J. Mater. Chem. A* **2013**, *1*, 13454. [CrossRef]
62. Zhao, Y.; Zhao, Y.; Feng, H.; Shen, J. Synthesis of Nickel Phosphide Nano-Particles in a Eutectic Mixture for Hydrotreating Reactions. *J. Mater. Chem.* **2011**, *21*, 8137. [CrossRef]
63. Zheng, H.; Gu, C.-D.; Wang, X.-L.; Tu, J.-P. Fast Synthesis and Optical Property of SnO Nanoparticles from Choline Chloride-Based Ionic Liquid. *J. Nanopart. Res.* **2014**, *16*, 2288. [CrossRef]
64. Xiong, Q.Q.; Tu, J.P.; Ge, X.; Wang, X.L.; Gu, C.D. One-Step Synthesis of Hematite Nanospindles from Choline Chloride/Urea Deep Eutectic Solvent with Highly Powerful Storage versus Lithium. *J. Power Sources* **2015**, *274*, 1–7. [CrossRef]
65. Ge, X.; Gu, C.D.; Wang, X.L.; Tu, J.P. Correlation between Microstructure and Electrochemical Behavior of the Mesoporous Co_3O_4 Sheet and Its Ionothermal Synthesized Hydrotalcite-like α-$Co(OH)_2$ Precursor. *J. Phys. Chem. C* **2014**, *118*, 911–923. [CrossRef]
66. Ge, X.; Gu, C.D.; Wang, X.L.; Tu, J.P. Endowing Manganese Oxide with Fast Adsorption Ability through Controlling the Manganese Carbonate Precursor Assembled in Ionic Liquid. *J. Colloid Interface Sci.* **2015**, *438*, 149–158. [CrossRef]
67. Lu, Y.-H.; Lin, W.-H.; Yang, C.-Y.; Chiu, Y.-H.; Pu, Y.-C.; Lee, M.-H.; Tseng, Y.-C.; Hsu, Y.-J. A Facile Green Antisolvent Approach to Cu^{2+}-Doped ZnO Nanocrystals with Visible-Light-Responsive Photoactivities. *Nanoscale* **2014**, *6*, 8796. [CrossRef]
68. Gu, C.; Zhang, H.; Wang, X.; Tu, J. One-Pot Synthesis of SnO_2/Reduced Graphene Oxide Nanocomposite in Ionic Liquid-Based Solution and Its Application for Lithium Ion Batteries. *Mater. Res. Bull.* **2013**, *48*, 4112–4117. [CrossRef]
69. Gu, C.D.; Xu, X.J.; Tu, J.P. Fabrication and Wettability of Nanoporous Silver Film on Copper from Choline Chloride-Based Deep Eutectic Solvents. *J. Phys. Chem. C* **2010**, *114*, 13614–13619. [CrossRef]
70. Zhang, H.; Lu, Y.; Gu, C.-D.; Wang, X.-L.; Tu, J.-P. Ionothermal Synthesis and Lithium Storage Performance of Core/Shell Structured Amorphous@crystalline Ni–P Nanoparticles. *CrystEngComm* **2012**, *14*, 7942. [CrossRef]
71. Abbott, A.P.; El Ttaib, K.; Ryder, K.S.; Smith, E.L. Electrodeposition of Nickel Using Eutectic Based Ionic Liquids. *Trans. IMF* **2008**, *86*, 234–240. [CrossRef]

72. Hou, Y.; Peng, Z.; Liang, J.; Fu, S. Ni–Ti Nanocomposite Coatings Electro-Codeposited from Deep Eutectic Solvent Containing Ti Nanoparticles. *J. Electrochem. Soc.* **2020**, *167*, 042502. [CrossRef]
73. Abbott, A.P.; Ttaib, K.E.; Frisch, G.; Ryder, K.S.; Weston, D. The Electrodeposition of Silver Composites Using Deep Eutectic Solvents. *Phys. Chem. Chem. Phys.* **2012**, *14*, 2443. [CrossRef]
74. Mota-Morales, J.D.; Gutiérrez, M.C.; Ferrer, M.L.; Jiménez, R.; Santiago, P.; Sanchez, I.C.; Terrones, M.; del Monte, F.; Luna-Bárcenas, G. Synthesis of Macroporous Poly(Acrylic Acid)–Carbon Nanotube Composites by Frontal Polymerization in Deep-Eutectic Solvents. *J. Mater. Chem. A* **2013**, *1*, 3970. [CrossRef]
75. Li, X.; Row, K.H. Preparation of Levofloxacin-Imprinted Nanoparticles Using Designed Deep Eutectic Solvents for the Selective Removal of *Levofloxacin* Pollutants from Environmental Waste Water. *Analyst* **2020**, *145*, 2958–2965. [CrossRef]
76. Zainal-Abidin, M.H.; Hayyan, M.; Ngoh, G.C.; Wong, W.F. From Nanoengineering to Nanomedicine: A Facile Route to Enhance Biocompatibility of Graphene as a Potential Nano-Carrier for Targeted Drug Delivery Using Natural Deep Eutectic Solvents. *Chem. Eng. Sci.* **2019**, *195*, 95–106. [CrossRef]
77. Mohammadpour, Z.; Abdollahi, S.H.; Safavi, A. Sugar-Based Natural Deep Eutectic Mixtures as Green Intercalating Solvents for High-Yield Preparation of Stable MoS_2 Nanosheets: Application to Electrocatalysis of Hydrogen Evolution Reaction. *ACS Appl. Energy Mater.* **2018**, *1*, 5896–5906. [CrossRef]
78. Karimi, M.; Jodaei, A.; Khajvandi, A.; Sadeghinik, A.; Jahandideh, R. In-Situ Capture and Conversion of Atmospheric CO_2 into Nano-$CaCO_3$ Using a Novel Pathway Based on Deep Eutectic Choline Chloride-Calcium Chloride. *J. Environ. Manag.* **2018**, *206*, 516–522. [CrossRef]
79. Adhikari, L.; Larm, N.E.; Bhawawet, N.; Baker, G.A. Rapid Microwave-Assisted Synthesis of Silver Nanoparticles in a Halide-Free Deep Eutectic Solvent. *ACS Sustain. Chem. Eng.* **2018**, *6*, 5725–5731. [CrossRef]
80. Adhikari, L.; Larm, N.E.; Baker, G.A. Argentous Deep Eutectic Solvent Approach for Scaling Up the Production of Colloidal Silver Nanocrystals. *ACS Sustain. Chem. Eng.* **2019**, *7*, 11036–11043. [CrossRef]
81. Adhikari, L.; Larm, N.E.; Baker, G.A. Batch and Flow Nanomanufacturing of Large Quantities of Colloidal Silver and Gold Nanocrystals Using Deep Eutectic Solvents. *ACS Sustain. Chem. Eng.* **2020**, *8*, 14679–14689. [CrossRef]
82. Wang, K.-Y.; Liu, H.-W.; Zhang, S.; Ding, D.; Cheng, L.; Wang, C. Selenidostannates and a Silver Selenidostannate Synthesized in Deep Eutectic Solvents: Crystal Structures and Thermochromic Study. *Inorg. Chem.* **2019**, *58*, 2942–2953. [CrossRef]
83. Antenucci, A.; Bonomo, M.; Ghigo, G.; Gontrani, L.; Barolo, C.; Dughera, S. How Do Arenediazonium Salts Behave in Deep Eutectic Solvents? A Combined Experimental and Computational Approach. *J. Mol. Liq.* **2021**, *339*, 116743. [CrossRef]
84. Li, X.; Row, K.H. Preparation of Deep Eutectic Solvent-Based Hexagonal Boron Nitride-Molecularly Imprinted Polymer Nanoparticles for Solid Phase Extraction of Flavonoids. *Microchim. Acta* **2019**, *186*, 753. [CrossRef]
85. Sun, Y.; Cheng, S.; Mao, Z.; Lin, Z.; Ren, X.; Yu, Z. High Electrochemical Activity of a Ti/SnO_2–Sb Electrode Electrodeposited Using Deep Eutectic Solvent. *Chemosphere* **2020**, *239*, 124715. [CrossRef]
86. Douglas, F.J.; MacLaren, D.A.; Murrie, M. A Study of the Role of the Solvent during Magnetite Nanoparticle Synthesis: Tuning Size, Shape and Self-Assembly. *RSC Adv.* **2012**, *2*, 8027. [CrossRef]
87. Das, L.; Koonathan, L.D.; Kunwar, A.; Neogy, S.; Debnath, A.K.; Adhikari, S. Nontoxic Photoluminescent Tin Oxide Nanoparticles for Cell Imaging: Deep Eutectic Solvent Mediated Synthesis, Tuning and Mechanism. *Mater. Adv.* **2021**, *2*, 4303–4315. [CrossRef]
88. Hammond, O.S.; Atri, R.S.; Bowron, D.T.; de Campo, L.; Diaz-Moreno, S.; Keenan, L.L.; Doutch, J.; Eslava, S.; Edler, K.J. Structural Evolution of Iron Forming Iron Oxide in a Deep Eutectic-Solvothermal Reaction. *Nanoscale* **2021**, *13*, 1723–1737. [CrossRef]
89. Exposito, A.J.; Barrie, P.J.; Torrente-Murciano, L. Fast Synthesis of CeO_2 Nanoparticles in a Continuous Microreactor Using Deep Eutectic Reline as Solvent. *ACS Sustain. Chem. Eng.* **2020**, *8*, 18297–18302. [CrossRef]
90. Mehrabi, N.; Abdul Haq, U.F.; Reza, M.T.; Aich, N. Application of Deep Eutectic Solvent for Conjugation of Magnetic Nanoparticles onto Graphene Oxide for Lead(II) and Methylene Blue Removal. *J. Environ. Chem. Eng.* **2020**, *8*, 104222. [CrossRef]
91. Chen, R.; Chen, J.; Ma, T.; Pan, C.; Kang, J.; Zou, H.; Yang, W.; Chen, S. Porous $NixCo_{2-x}(OH)_3Cl$ Nanoparticles as Cathode Materials for Hybrid Supercapacitor. *J. Energy Storage* **2021**, *47*, 103655. [CrossRef]
92. Nazari, F.; Tabaraki, R. Sensitive Fluorescence Detection of Atorvastatin by Doped Carbon Dots Synthesized in Deep Eutectic Media. *Spectrochim. Acta Part A Mol. Biomol. Spectrosc.* **2020**, *236*, 118341. [CrossRef]
93. Zhang, J.; Wang, Z.; Chen, R.; Chen, F. New Soft Chemistry Route to Titanomagnetite Magnetic Nanoparticles with Enhanced Peroxidase-like Activity. *Powder Technol.* **2020**, *373*, 39–45. [CrossRef]
94. Morales Betancourt, A.L.; Smith, C.; Minor, K.; Christodoulou, A.; Naranjo, J.; Tek, S.; Nash, K. Synthesis of Colloidal SeTe Nanoalloy by Pulsed Laser Ablation in Deep Eutectic Solvents to Be Used as Anticancer Treatment. In Proceedings of the Colloidal Nanoparticles for Biomedical Applications XVI, San Antonio, TX, USA, 12 March 2021. [CrossRef]
95. Jia, H.; Sun, J.; Dong, M.; Dong, H.; Zhang, H.; Xie, X. Deep Eutectic Solvent Electrolysis for Preparing Water-Soluble Magnetic Iron Oxide Nanoparticles. *Nanoscale* **2021**, *13*, 19004–19011. [CrossRef]
96. Edison, T.N.J.I.; Atchudan, R.; Karthik, N.; Chandrasekaran, S.; Perumal, S.; Raja, P.B.; Perumal, V.; Lee, Y.R. Deep Eutectic Solvent Assisted Electrosynthesis of Ruthenium Nanoparticles on Stainless Steel Mesh for Electrocatalytic Hydrogen Evolution Reaction. *Fuel* **2021**, *297*, 120786. [CrossRef]
97. Juárez-Marmolejo, L.; Maldonado-Teodocio, B.; de Oca-Yemha, M.G.M.; Romero-Romo, M.; Arce-Estrada, E.M.; Ezeta-Mejía, A.; Ramírez-Silva, M.T.; Mostany, J.; Palomar-Pardavé, M. Electrocatalytic Oxidation of Formic Acid by Palladium Nanoparticles Electrochemically Synthesized from a Deep Eutectic Solvent. *Catal. Today* 2021. [CrossRef]

98. Dang, T.K.; van Toan, N.; Hung, C.M.; van Duy, N.; Viet, N.N.; Thong, L.V.; Son, N.T.; van Hieu, N.; le Manh, T. Investigation of Zinc Electronucleation and Growth Mechanisms onto Platinum Electrode from a Deep Eutectic Solvent for Gas Sensing Applications. *J. Appl. Electrochem.* **2022**, *52*, 299–309. [CrossRef]
99. Phuong, T.D.V.; Phi, T.-L.; Phi, B.H.; van Hieu, N.; Tang Nguyen, S.; le Manh, T. Electrochemical Behavior and Electronucleation of Copper Nanoparticles from $CuCl_2 \cdot 2H_2O$ Using a Choline Chloride-Urea Eutectic Mixture. *J. Nanomater.* **2021**, *2021*, 9619256. [CrossRef]
100. El-Hallag, I.; Elsharkawy, S.; Hammad, S. Electrodeposition of Ni Nanoparticles from Deep Eutectic Solvent and Aqueous Solution as Electrocatalyst for Methanol Oxidation in Acidic Media. *Int. J. Hydrogen Energy* **2021**, *46*, 15442–15453. [CrossRef]
101. Zhang, Y.; Ru, J.; Hua, Y.; Huang, P.; Bu, J.; Wang, Z. Facile and Controllable Synthesis of NiS_2 Nanospheres in Deep Eutectic Solvent. *Mater. Lett.* **2021**, *283*, 128742. [CrossRef]
102. da Silva, W.; Queiroz, A.C.; Brett, C.M.A. Nanostructured Poly(Phenazine)/Fe_2O_3 Nanoparticle Film Modified Electrodes Formed by Electropolymerization in Ethaline-Deep Eutectic Solvent. Microscopic and Electrochemical Characterization. *Electrochim. Acta* **2020**, *347*, 136284. [CrossRef]
103. Rastbood, S.; Hadjmohammadi, M.R.; Majidi, S.M. Development of a Magnetic Dispersive Micro-Solid-Phase Extraction Method Based on a Deep Eutectic Solvent as a Carrier for the Rapid Determination of Meloxicam in Biological Samples. *Anal. Methods* **2020**, *12*, 2331–2337. [CrossRef]
104. Hou, Y.; Peng, Z.; Liang, J.; Liu, M. Ni-Al Nanocomposite Coating Electrodeposited from Deep Eutectic Solvent. *Surf. Coat. Technol.* **2021**, *405*, 126587. [CrossRef]
105. Wang, X.; Sun, M.; Xiang, S.; Waqas, M.; Fan, Y.; Zhong, J.; Huang, K.; Chen, W.; Liu, L.; Yang, J. Template-Free Synthesis of Platinum Hollow-Opened Structures in Deep-Eutectic Solvents and Their Enhanced Performance for Methanol Electrooxidation. *Electrochim. Acta* **2020**, *337*, 135742. [CrossRef]
106. Lei, H.; Singh Siwal, S.; Zhang, X.; Zhang, Q. Compositional and Morphological Engineering of In-Situ-grown Ag Nanoparticles on Cu Substrate for Enhancing Oxygen Reduction Reaction Activity: A Novel Electrochemical Redox Tuning Approach. *J. Colloid Interface Sci.* **2020**, *571*, 1–12. [CrossRef]
107. Albayati, N.; Kadhom, M. Preparation of Functionalised UiO-66 Metal–Organic Frameworks (MOFs) Nanoparticles Using Deep Eutectic Solvents as a Benign Medium. *Micro Nano Lett.* **2020**, *15*, 1075–1078. [CrossRef]
108. Leal-Duaso, A.; Mayoral, J.A.; Pires, E. Steps Forward toward the Substitution of Conventional Solvents in the Heck–Mizoroki Coupling Reaction: Glycerol-Derived Ethers and Deep Eutectic Solvents as Reaction Media. *ACS Sustain. Chem. Eng.* **2020**, *8*, 13076–13084. [CrossRef]
109. Jin, X.; Ma, Z.; Liu, G.; Hu, D.; Song, C.; Huang, Q. In-Situ Ionothermal Precipitation of Well-Dispersed ZnO Nanoparticles onto 2-Dimension Neat Graphene Sheets with Excellent Photocatalytic Activity. *J. Environ. Chem. Eng.* **2020**, *8*, 104030. [CrossRef]
110. Mitar, A.; Prlić Kardum, J. Intensification of Mass Transfer in the Extraction Process with a Nanofluid Prepared in a Natural Deep Eutectic Solvent. *Chem. Eng. Technol.* **2020**, *43*, 2286–2294. [CrossRef]
111. Li, W.; Zhao, X.; Huang, T.; Ren, Y.; Gong, W.; Guo, Y.; Wang, J.; Tu, Q. Preparation of Sodium Hyaluronate/Dopamine/AgNPs Hydrogel Based on the Natural Eutetic Solvent as an Antibaterial Wound Dressing. *Int. J. Biol. Macromol.* **2021**, *191*, 60–70. [CrossRef]
112. Li, H.; Wang, Y.; He, X.; Chen, J.; Xu, F.; Liu, Z.; Zhou, Y. A Green Deep Eutectic Solvent Modified Magnetic Titanium Dioxide Nanoparticles for the Solid-Phase Extraction of Chymotrypsin. *Talanta* **2021**, *230*, 122341. [CrossRef]
113. Li, D.; Huang, Y.; Li, Z.; Zhong, L.; Liu, C.; Peng, X. Deep Eutectic Solvents Derived Carbon-Based Efficient Electrocatalyst for Boosting H2 Production Coupled with Glucose Oxidation. *Chem. Eng. J.* **2022**, *430*, 132783. [CrossRef]
114. Iwanow, M.; Seidler, J.; Vieira, L.; Kaiser, M.; van Opdenbosch, D.; Zollfrank, C.; Gärtner, T.; Richter, M.; König, B.; Sieber, V. Enhanced C2 and C3 Product Selectivity in Electrochemical CO_2 Reduction on Carbon-Doped Copper Oxide Catalysts Prepared by Deep Eutectic Solvent Calcination. *Catalysts* **2021**, *11*, 542. [CrossRef]
115. Baby, J.N.; Sriram, B.; Wang, S.-F.; George, M. Effect of Various Deep Eutectic Solvents on the Sustainable Synthesis of $MgFe_2O_4$ Nanoparticles for Simultaneous Electrochemical Determination of Nitrofurantoin and 4-Nitrophenol. *ACS Sustain. Chem. Eng.* **2020**, *8*, 1479–1486. [CrossRef]
116. Meng, J.; Liu, Y.; Shi, X.; Chen, W.; Zhang, X.; Yu, H. Recyclable Nanocellulose-Confined Palladium Nanoparticles with Enhanced Room-Temperature Catalytic Activity and Chemoselectivity. *Sci. China Mater.* **2021**, *64*, 621–630. [CrossRef]
117. Ying, H.; Chen, T.; Zhang, C.; Bi, J.; Li, Z.; Hao, J. Regeneration of Porous Fe_3O_4 Nanosheets from Deep Eutectic Solvent for High-Performance Electrocatalytic Nitrogen Reduction. *J. Colloid Interface Sci.* **2021**, *602*, 64–72. [CrossRef]
118. Wadekar, P.H.; Ghosh, A.; Khose, R.V.; Pethsangave, D.A.; Mitra, S.; Some, S. A Novel Chemical Reduction/Co-Precipitation Method to Prepare Sulfur Functionalized Reduced Graphene Oxide for Lithium-Sulfur Batteries. *Electrochim. Acta* **2020**, *344*, 136147. [CrossRef]
119. Jamshidi, F.; Nouri, N.; Sereshti, H.; Shojaee Aliabadi, M.H. Synthesis of Magnetic Poly (Acrylic Acid-Menthol Deep Eutectic Solvent) Hydrogel: Application for Extraction of Pesticides. *J. Mol. Liq.* **2020**, *318*, 114073. [CrossRef]
120. Vallejo-Macías, M.T.; Recio-Colmenares, C.L.; Pelayo-Vázquez, J.B.; Gómez-Salazar, S.; Carvajal-Ramos, F.; Soltero-Martínez, J.F.; Vázquez-Lepe, M.; Mota-Morales, J.D.; Pérez-García, M.G. Macroporous Polyacrylamide γ-Fe_2O_3 Nanoparticle Composites as Methylene Blue Dye Adsorbents. *ACS Appl. Nano Mater.* **2020**, *3*, 5794–5806. [CrossRef]

121. Deng, Y.; Ouyang, J.; Wang, H.; Yang, C.; Zhu, Y.; Wang, J.; Li, D.; Ma, K. Magnetic Nanoparticles Prepared in Natural Deep Eutectic Solvent for Enzyme Immobilisation. *Biocatal. Biotransform.* **2021**, 1–11. [CrossRef]
122. Sakthi Sri, S.P.; Taj, J.; George, M. Facile Synthesis of Magnetite Nanocubes Using Deep Eutectic Solvent: An Insight to Anticancer and Photo-Fenton Efficacy. *Surf. Interfaces* **2020**, *20*, 100609. [CrossRef]
123. Bide, Y.; Shokrollahzadeh, S. Toward Tailoring of a New Draw Solute for Forward Osmosis Process: Branched Poly (Deep Eutectic Solvent)-Decorated Magnetic Nanoparticles. *J. Mol. Liq.* **2020**, *320*, 114409. [CrossRef]
124. Wei, X.; Wang, Y.; Chen, J.; Xu, F.; Liu, Z.; He, X.; Li, H.; Zhou, Y. Adsorption of Pharmaceuticals and Personal Care Products by Deep Eutectic Solvents-Regulated Magnetic Metal-Organic Framework Adsorbents: Performance and Mechanism. *Chem. Eng. J.* **2020**, *392*, 124808. [CrossRef]
125. Chen, Y.; Zhang, S.; Xue, Y.; Mo, L.; Zhang, Z. Palladium Anchored on a Covalent Organic Framework as a Heterogeneous Catalyst for Phosphorylation of Aryl Bromides. *Appl. Organomet. Chem.* **2022**, *36*, e6480. [CrossRef]
126. Iqbal, J.; Shah, N.S.; Sayed, M.; Muhammad, N.; Rehman, S.; Khan, J.A.; Haq Khan, Z.U.; Howari, F.M.; Nazzal, Y.; Xavier, C.; et al. Deep Eutectic Solvent-Mediated Synthesis of Ceria Nanoparticles with the Enhanced Yield for Photocatalytic Degradation of Flumequine under UV-C. *J. Water Process Eng.* **2020**, *33*, 101012. [CrossRef]
127. Iqbal, J.; Shah, N.S.; Sayed, M.; Ali Khan, J.; Muhammad, N.; Khan, Z.U.H.; Rehman, S.U.; Naseem, M.; Howari, F.M.; Nazzal, Y.; et al. Synthesis of Nitrogen-Doped Ceria Nanoparticles in Deep Eutectic Solvent for the Degradation of Sulfamethaxazole under Solar Irradiation and Additional Antibacterial Activities. *Chem. Eng. J.* **2020**, *394*, 124869. [CrossRef]
128. Dehury, P.; Mahanta, U.; Banerjee, T. Comprehensive Assessment on the Use of Boron Nitride-Based Nanofluids Comprising Eutectic Mixtures of Diphenyl Ether and Menthol for Enhanced Thermal Media. *ACS Sustain. Chem. Eng.* **2020**, *8*, 14595–14604. [CrossRef]
129. Qin, H.; Hu, X.; Wang, J.; Cheng, H.; Chen, L.; Qi, Z. Overview of Acidic Deep Eutectic Solvents on Synthesis, Properties and Applications. *Green Energy Environ.* **2020**, *5*, 8–21. [CrossRef]
130. Eweka, E.I.; Kerridge, D.H. Solution Chemistry of Molten Amide-Nitrate Eutectics. *Chem. Pap.* **1999**, *53*, 11–15.
131. Mackowiak, A.; Galek, P.; Fic, K. Deep Eutectic Solvents for High-Temperature Electrochemical Capacitors. *ChemElectroChem* **2021**, *8*, 4028–4037. [CrossRef]
132. Taghavi, S.; Amoozadeh, A.; Nemati, F. Deep Eutectic Solvent-assisted Synthesis of Highly Efficient Nanocatalyst (N-TiO_2@TDI@DES ($ZnCl_2$:Urea)) for Chemoselective Oxidation of Sulfides to Sulfoxides. *Appl. Organomet. Chem.* **2021**, *35*, e6127. [CrossRef]
133. Taghavi, S.; Amoozadeh, A.; Nemati, F. The First Report of Deep Eutectic Solvent (DES) Nano-photocatalyst (N-TiO_2-P25@TDI@DES (Urea: $ZnCl_2$)) and Its Application on Selective Oxidation of Benzyl Alcohols to Benzaldehydes. *J. Chem. Technol. Biotechnol.* **2021**, *96*, 384–393. [CrossRef]
134. Riadi, Y.; Geesi, M.H.; Ouerghi, O.; Dehbi, O.; Elsanousi, A.; Azzallou, R. Synergistic Catalytic Effect of the Combination of Deep Eutectic Solvents and Hierarchical H-TiO_2 Nanoparticles toward the Synthesis of Benzimidazole-Linked Pyrrolidin-2-One Heterocycles: Boosting Reaction Yield. *Polycycl. Aromat. Compd.* **2021**, 1–15. [CrossRef]
135. Nguyen, T.T.; Tran, P.H. One-Pot Multicomponent Synthesis of Thieno [2,3-*b*]Indoles Catalyzed by a Magnetic Nanoparticle-Supported $[Urea]_4$ $[ZnCl_2]$ Deep Eutectic Solvent. *RSC Adv.* **2020**, *10*, 9663–9671. [CrossRef]
136. Hammond, O.S.; Bowron, D.T.; Edler, K.J. Structure and Properties of "Type IV" Lanthanide Nitrate Hydrate:Urea Deep Eutectic Solvents. *ACS Sustain. Chem. Eng.* **2019**, *7*, 4932–4940. [CrossRef]
137. Gupta, R.; Gamare, J.; Sahu, M.; Pandey, K.; Gupta, S.K. Electrochemical and Thermodynamic Insights on Actinide Type (IV) Deep Eutectic Solvent. *J. Mol. Liq.* **2021**, *329*, 115550. [CrossRef]
138. Xu, L.-H.; Ma, C.-Y.; Zhang, C.; Liu, J.; Peng, X.-P.; Yao, S.-Q.; Min, D.-Y.; Yuan, T.-Q.; Wen, J.-L. Ultrafast Fractionation of Wild-Type and CSE down-Regulated Poplars by Microwave-Assisted Deep Eutectic Solvents (DES) for Cellulose Bioconversion Enhancement and Lignin Nanoparticles Fabrication. *Ind. Crops Prod.* **2022**, *176*, 114275. [CrossRef]
139. Luo, T.; Wang, C.; Ji, X.; Yang, G.; Chen, J.; Yoo, C.G.; Janaswamy, S.; Lyu, G. Innovative Production of Lignin Nanoparticles Using Deep Eutectic Solvents for Multifunctional Nanocomposites. *Int. J. Biol. Macromol.* **2021**, *183*, 781–789. [CrossRef]
140. Guo, Y.; Xu, L.; Shen, F.; Hu, J.; Huang, M.; He, J.; Zhang, Y.; Deng, S.; Li, Q.; Tian, D. Insights into Lignocellulosic Waste Fractionation for Lignin Nanospheres Fabrication Using Acidic/Alkaline Deep Eutectic Solvents. *Chemosphere* **2022**, *286*, 131798. [CrossRef]
141. Luo, T.; Wang, C.; Ji, X.; Yang, G.; Chen, J.; Janaswamy, S.; Lyu, G. Preparation and Characterization of Size-Controlled Lignin Nanoparticles with Deep Eutectic Solvents by Nanoprecipitation. *Molecules* **2021**, *26*, 218. [CrossRef]
142. Tian, D.; Guo, Y.; Huang, M.; Zhao, L.; Deng, S.; Deng, O.; Zhou, W.; Hu, J.; Shen, F. Bacterial Cellulose/Lignin Nanoparticles Composite Films with Retarded Biodegradability. *Carbohydr. Polym.* **2021**, *274*, 118656. [CrossRef] [PubMed]
143. Bryant, S.J.; da Silva, M.A.; Hossain, K.M.Z.; Calabrese, V.; Scott, J.L.; Edler, K.J. Deep Eutectic Solvent in Water Pickering Emulsions Stabilised by Cellulose Nanofibrils. *RSC Adv.* **2020**, *10*, 37023–37027. [CrossRef]